

Chapter 1

Astrophysical aspects of general relativistic mass twin stars

David Blaschke^{1,2,3}, David Edwin Alvarez-Castillo¹,
Alexander Ayriyan^{4,5}, Hovik Grigorian^{4,5,6}, Noshad Khosravi Lagarni^{1,7},
Fridolin Weber^{8,9}

¹ *Bogoliubov Laboratory for Theoretical Physics, Joint Institute for Nuclear Research, Joliot-Curie street 6, 141980 Dubna, Russia*

² *Institute of Theoretical Physics, University of Wroclaw, Max Born place 9, 50-204 Wroclaw, Poland*

³ *National Research Nuclear University (MEPhI), Kashirskoe Shosse 31, 115409 Moscow, Russia*

⁴ *Laboratory for Information Technologies, Joint Institute for Nuclear Research, Joliot-Curie street 6, 141980 Dubna, Russia*

⁵ *Computational Physics and IT Division, A.I. Alikhanyan National Science Laboratory, Alikhanyan Brothers street 2, 0036 Yerevan, Armenia*

⁶ *Department of Physics, Yerevan State University, Alek Manukyan street 1, 0025 Yerevan, Armenia*

⁷ *Department of Physics, Alzahra University, Tehran, 1993893973, Iran*

⁸ *Department of Physics, San Diego State University, 5500 Campanile Drive, San Diego, CA 92182, USA*

⁹ *Center for Astrophysics and Space Sciences, University of California, San Diego, La Jolla, CA 92093, USA*

Abstract. In this chapter we will introduce an effective equation of state (EoS) model based on polytropes that serves to study the so called "mass twins" scenario, where two compact stars have approximately the same mass but (significant for observation) quite different radii. Stellar mass twin configurations are obtained if a strong first-order phase transition occurs in the interior of a compact star. In the mass-radius diagram of compact stars, this will lead to a third branch of gravitationally stable stars with features that are very distinctive from those of white dwarfs and neutron stars. We discuss rotating hybrid star sequences in the slow rotation approximation and in full general relativity and draw conclusions for an upper limit on the maximum mass of nonrotating compact stars that has recently be deduced from the observation of the merger event GW170817.

1.1 Introduction

Compact stars, the stellar remnants following the death of main sequence stars, have been the subject of investigation since the beginning of the last century. In particular, the determination of the internal composition of neutron stars is an open problem. Researching it involves many areas of physics, like nuclear, plasma, particle physics and relativistic astrophysics. Moreover, due to the enormous compactness (as expressed in the mass-radius ratio) of compact stars, these objects are extremely relativistic. Therefore, one can neither exclusively apply non-relativistic quantum mechanics nor classical Newtonian gravity to describe the observational properties of compact stars.

During the last decade important astronomical observations have shed light onto the nature of the dense, cold matter in the stellar interiors of compact stars. The detection of massive neutron stars, of about $2M_{\odot}$, has constrained the maximum density values in their cores and also revealed the stiff nature of the nuclear equation of state (EoS) at ultra-high densities. Strongly related to this issue, and one of the most interesting aspects of modern dense-matter physics, concerns the possible onset of quark deconfinement in the cores of compact stars.

Microscopic models that take into account the nuclear interactions either at the nucleon or quark level aim at providing a realistic hadronic or

quark matter EoS, respectively. Neutron star matter must be thermodynamically consistent. Interestingly, due to the fast cooling of neutron stars after their birth in a supernova collapse the thermal contributions to the EoS do not contribute substantially and can safely be neglected [Yakovlev *et al.* (2001)]. The thermodynamic system can therefore be described by three macroscopic variables: energy density ε , baryonic density n , and pressure P . A fourth quantity of great interest, the chemical potential, can then be obtained as $\mu = (P + \varepsilon)/n$.

In addition, the most basic conditions that the system must fulfill include global charge neutrality and β -equilibrium. The latter is derived from the reaction balance of beta decay and its inverse, the electron capture, due to the weak interactions and fixes the relation between the chemical potentials of different species in the system.

With the above conditions satisfied, the neutron star equation of state becomes an expression of the form $P(\varepsilon)$, where $\varepsilon = \varepsilon(n)$ and $P = P(n)$ acquire parametric forms. Furthermore, in order to compute the internal properties of compact stars, it is necessary to obtain internal pressure profiles. This will result in mass-radius relations that characterize an EoS. Neutron stars are extremely relativistic objects which require to be treated within Einstein's general theory of relativity rather than simply Newtonian gravity, which may still be applicable to white dwarf stars. In this sense, our contribution addresses "strong gravity" in a unique fashion. To give an example, for a pulsar of mass $M = 2 M_{\odot}$ with a typical radius of around 12 km, the general relativistic correction factor amounts to $1/(1 - 2GM/R) = 2$ [Tolman (1939); Oppenheimer and Volkoff (1939)], which is a 100% correction relative to Newtonian gravity!

In the following sections we will introduce an effective EoS model based on polytropes (Alvarez-Castillo and Blaschke, 2017) that serves to study the so called "mass twins" scenario, where two compact stars have approximately the same mass but (significant for observation) quite different radii [Glendenning and Kettner (2000)]. Stellar mass twin configurations are obtained if a strong first-order phase transition occurs in the interior of a compact star. In the mass-radius diagram of compact stars, this will lead to a third branch of gravitationally stable stars with features that are very distinctive from those of white dwarfs and neutron stars. The condition on the EoS that will lead to mass twins was first derived by Seidov (Seidov, 1971), see also (Schaeffer *et al.*, 1983; Lindblom, 1998), namely that the central energy density ε_v , central pressure P_c , and the jump in energy

associated with the phase transition $\Delta\varepsilon$ obey the relation

$$\frac{\Delta\varepsilon}{\varepsilon_c} \geq \frac{1}{2} + \frac{3}{2} \frac{P_c}{\varepsilon_c}. \quad (1.1)$$

When fulfilled, the corresponding compact star will suffer an instability of the same type as the maximum mass star of a stellar sequence. Most interestingly, stars with central densities higher than the density of the maximum-mass star become stable again if their gravitational masses obey $\partial M/\partial\varepsilon_c(0) > 0$, thereby populating a third branch with stable mass twins.

1.2 Self-consistent set of field equations for stationary rotating and tidally deformed stars

The geometrical description of the space-time structure curved due to the mass-energy of a compact star is given by the general metric form defining the interval between the infinitesimally close events,

$$ds^2 = g_{\mu\nu}(x)dx^\mu dx^\nu. \quad (1.2)$$

The curvature of the space-time is satisfying the Einstein field equations $G_\nu^\mu = 8\pi G T_\nu^\mu$, where $G_\nu^\mu = R_\nu^\mu - 1/2\delta_\nu^\mu R$. Here R_ν^μ is the Ricci curvature tensor and R the scalar curvature. On the right hand side of the Einstein equation we have the energy-momentum tensor T_ν^μ of the stellar matter and G is the gravitational constant ($\hbar = c = 1$).

The metric tensor $g_{\mu\nu}(x)$ has the same symmetry as the matter distribution. Therefore, if one assumes that the star is static and not deformed the metric tensor is diagonal and depends only on the distance from the center of the star. In the case of stationary rotating stars the symmetry of the matter will be axial symmetric. In this case due to the rotational motion of the star the non-diagonal element $g_{t\phi}$ (t -time coordinate, ϕ - azimuthal angle of the spherical coordinate system) will not be zero in the inertial frames connected with the star. The existence of such a term leads to the Lense-Thirring effect of frame dragging for the motion of bodies in the gravitational field of rotating compact relativistic stellar objects. However, in the case of small but static deformations the metric will be non-spherical but diagonal.

1.2.1 Einstein equations for axial symmetry

The general form of the metric for an axially symmetric space-time manifold in the inertial frame where the star center is at rest is

$$ds^2 = e^{\nu(r,\theta)} dt^2 - e^{\lambda(r,\theta)} dr^2 - r^2 e^{\mu(r,\theta)} [d\theta^2 + \sin^2 \theta (d\phi + \omega(r, \theta) dt)^2], \quad (1.3)$$

where a spherically symmetric coordinate system has been used in order to obtain the Schwarzschild solution as a limiting case. This line element is time - translation and axial-rotational invariant; all metric functions are dependent on the coordinate distance from the coordinate center r and altitude angle θ between the radius vector and the axis of symmetry.

The energy momentum tensor of stellar matter can be approximated by the expression of the energy momentum tensor of an ideal fluid

$$T^\nu_\mu = (\varepsilon + P) u_\mu u^\nu - P \delta^\nu_\mu, \quad (1.4)$$

where u^μ is the 4-velocity of matter, P the pressure and ε the energy density.

Once the energy-momentum tensor (1.4) is fixed by the choice of the equation of state for stellar matter, the unknown metric functions $\nu, \lambda, \mu, \bar{\omega}$ can be determined by the set of Einstein field equations for which we use the following four combinations.

There are three Einstein equations for the determination of the diagonal elements of the metric tensor,

$$G_r^r - G_t^t = 8\pi G (T_r^r - T_t^t), \quad (1.5)$$

$$G_\theta^\theta + G_\phi^\phi = 8\pi G (T_\theta^\theta + T_\phi^\phi), \quad (1.6)$$

$$G_\theta^r = 0, \quad (1.7)$$

and one for the determination of the non-diagonal element

$$G_\phi^t = 8\pi G T_\phi^t. \quad (1.8)$$

We use also one equation for the hydrodynamic equilibrium (Euler equation)

$$H(r, \theta) \equiv \int \frac{dP'}{P' + \varepsilon'} = \frac{1}{2} \ln[u^t(r, \theta)] + \text{const}, \quad (1.9)$$

where the gravitational enthalpy H thus introduced is a function of the energy and/or pressure distribution.

1.2.2 Full solution for uniform rotational bodies

In this section we describe the method of solution employed by the RNS code written by Stergioulas and Friedman (1995), based on the method developed by Komatsu *et al.* (1989) that also includes modifications by Cook *et al.* (1994). In addition, the inclusion of quadrupole moments is due to Morsink based on the method by Laarakkers and Poisson (1999).

In order to study the full solutions for rotating compact stars the following metric is considered [Cook *et al.* (1994)]:

$$ds^2 = -e^{\gamma(r,\theta)+\rho(r,\theta)} dt^2 + e^{2\alpha(r,\theta)} (dr^2 + r^2 d\theta^2) + e^{\gamma(r,\theta)-\rho(r,\theta)} r^2 \sin^2 \theta \times (d\phi - \omega(r,\theta)dt)^2, \quad (1.10)$$

which just like Eq. (1.3) properly describes a stationary, axisymmetric spacetime. In addition, the matter source is chosen to be a perfect fluid described by the stress energy tensor $T^{\mu\nu} = (\epsilon + P)u^\mu u^\nu + Pg^{\mu\nu}$, where u^μ is the four-velocity of matter. Three of the solutions to the gravitational field equations are found by a Green function approach therefore leading to the determination of the metric potentials ρ , γ and ω in term of integrals, whereas the α potential is found by solving a linear differential equation. Therefore, we find the corresponding numerical solutions to our compact star models by employing the RNS code. In the formulation of the problem, all the physical variables are written in dimensionless form by means of a fundamental length scale $\sqrt{\kappa}$, where $\kappa \equiv \frac{c^2}{G\epsilon_0}$ with $\epsilon_0 \equiv 10^{15} \text{g cm}^{-3}$.

Table 1.1 Dimensionless physical parameters of the gravitational field equations used in the RNS code formulation.

\bar{r}	\bar{t}	$\bar{\omega}$	$\bar{\Omega}$	$\bar{\rho}_0$	$\bar{\epsilon}$	\bar{P}	\bar{J}	\bar{M}
$\kappa^{-1/2} r$	$\kappa^{-1/2} ct$	$\kappa^{1/2} \frac{1}{c} \omega$	$\kappa^{1/2} \frac{1}{c} \Omega$	$\kappa \frac{G}{c^2} \rho_0$	$\kappa \frac{G}{c^2} \epsilon$	$\kappa \frac{G}{c^4} P$	$\kappa^{-1} \frac{G}{c^3} J$	$\kappa^{-1/2} \frac{G}{c^2} M$

The global parameters of the star are computed by means of the following expressions:

Table 1.2 Output parameters of the RNS code.

Gravitational mass-energy	M/M_\odot
Rest mass	M_0/M_\odot
Circumferencial radius [km]	R_e
Eccentricity	e
Central energy density [10^{15} g cm $^{-3}$]	ϵ_c
Angular velocity measured at infinity [10^3 s $^{-1}$]	Ω
Total angular momentum	cJ/GM_\odot^2
Rotational kinetic energy over gravitational energy	T/W
Measure of frame dragging	ω_c/Ω_c
Polar redshift	Z_p
Equatorial redshift in backward direction	Z_b
Equatorial redshift in forward direction	Z_f
Circumferential height of corotating marginally stable orbit [km]	h_+
Circumferential height of counterrotating marginally stable orbit [km]	h_+

$$M = \frac{4\pi\kappa^{1/2}c^2\bar{r}_e^3}{G} \int_0^1 \frac{s^2 ds}{(1-s)^4} \int_0^1 d\mu e^{2\alpha+\gamma} \times \left\{ \frac{\bar{\epsilon} + \bar{P}}{1-v^2} \left[1 + v^2 + \frac{2sv}{1-s} (1-\mu)^{1/2} \hat{\omega} e^{-\rho} \right] + 2\bar{P} \right\}, \quad (1.11)$$

$$M_0 = \frac{4\pi\kappa^{1/2}c^2\bar{r}_e^3}{G} \int_0^1 \frac{s^2 ds}{(1-s)^4} \int_0^1 d\mu e^{2\alpha+(\gamma-\rho)/2} \frac{\bar{\rho}_0}{(1-v^2)^{1/2}}, \quad (1.12)$$

$$J = \frac{4\pi\kappa c^3 \bar{r}_e^4}{G} \int_0^1 \frac{s^3 ds}{(1-s)^5} \int_0^1 d\mu (1-\mu^2)^{1/2} e^{2\alpha+\gamma-\rho} (\bar{\epsilon} + \bar{P}) \frac{v}{1-v^2}, \quad (1.13)$$

$$T = \frac{2\pi\kappa^{1/2}c^2\bar{r}_e^3}{G} \int_0^1 \frac{s^3 ds}{(1-s)^5} \int_0^1 d\mu (1-\mu^2)^{1/2} e^{2\alpha+\gamma-\rho} (\bar{\epsilon} + \bar{P}) \frac{v\hat{\Omega}}{1-v^2}, \quad (1.14)$$

where $\hat{\omega} \equiv \bar{r}_e \bar{\omega}$ and $\hat{\Omega} \equiv \bar{r}_e \bar{\Omega}$ with \bar{r}_e as the coordinate radius of the equator. Moreover, all the resulting quantities can be written in terms of the auxiliary variables μ and s , defined as $\mu \equiv \theta$ and $\bar{r} \equiv \bar{r}_e \left(\frac{s}{1-s} \right)$, respectively. Consequently, the four metric functions acquire a dependence on the above variables: $\rho(s, \mu)$, $\gamma(s, \mu)$, $\omega(s, \mu)$, $\alpha(s, \mu)$. The remaining quantities are:

$$R_e = \kappa^{1/2} \bar{r}_e e^{(\gamma_e - \rho_e)/2}, \quad (1.15)$$

$$Z_p = e^{-(\gamma_p + \rho_p)/2} - 1, \quad (1.16)$$

$$Z_f = \left(\frac{1-v_e}{1+v_e} \right)^{1/2} \frac{e^{-(\gamma_e + \rho_e)/2}}{1 + \hat{\omega}_e e^{-\rho_e}} - 1, \quad (1.17)$$

$$Z_b = \left(\frac{1 + v_e}{1 - v_e} \right)^{1/2} \frac{e^{-(\gamma_e + \rho_e)/2}}{1 - \hat{\omega}_e e^{-\rho_e}} - 1. \quad (1.18)$$

where the subscripts e and p denote evaluation at the equation and at the pole, respectively.

For the solutions of maximally rotating compact stars in numerical general relativity the version of RNS code has been employed which was available for download by the time of the writing of this contribution from the website <http://www.gravity.phys.uwm.edu/rns/>

1.2.3 Perturbation approach to the solution

The problem of the rotation can be solved iteratively by using a perturbation expansion of the metric tensor and the physical quantities in a Taylor series with respect to a small positive parameter β . As such a parameter for the perturbation expansion we use a dimensionless quantity. One of possible physically motivated way is to take the ratio of the rotational or deformation energy to the gravitational one. The gravitational energy could be estimated for a homogeneous Newtonian star as $\beta = E_{\text{def}}/E_{\text{grav}}$. In case of rotating stars the deformability is connected with the induced centrifugal force and the expansion parameter is $\beta = E_{\text{rot}}/E_{\text{grav}} = (\Omega/\Omega_0)^2$, where $\Omega_0^2 = 4\pi G\rho(0)$ with the mass density $\rho(0)$ at the center of the star. The choice of this parameter could be also motivated with the conditions when the problem is discussed. For example since for the stationary rotating stars can not have too high value of the angular velocity, because of mass shedding on Keplerian angular velocity $\Omega_K = \sqrt{GM/R_e^3}$ for the star with total mass M and R_e equatorial radius, the expansion gives sufficiently correct solutions already at $O(\Omega^2)$. So the expansion parameter is naturally limited to values $\Omega/\Omega_0 \ll 1$ by this condition of mechanical stability of the rigid rotation, because always $\Omega < \Omega_K = \Omega_0/\sqrt{3}$. This condition is fulfilled not only for homogeneous Newtonian spherical stars but also for the relativistic configurations even with a possible hadron-quark (deconfinement) transition, which we are going to discuss later in this chapter, see Fig. 1.6 below. The perturbation approach to slowly rotating stars has been developed first by Hartle (1967); Hartle and Thorne (1968), and independently by Sedrakyan and Chubaryan (1968b,a) and is described in detail in Refs. [Weber, F. (1999); Glendenning, N. K. (2000); Chubarian *et al.* (2000)]. Our notation and derivation in this section will follow Chubarian *et al.* (2000) while numerical solutions for the slow rotation (Ω^2 -) approximation are obtained with a code based on the improved Hartle scheme

[Weber and Glendenning (1992)].

The expansion of the metric tensor in a perturbation series with respect to the slow rotation parameter β can be expressed as

$$g_{\mu\nu}(r, \theta) = \sum_{j=0}^{\infty} (\sqrt{\beta})^j g_{\mu\nu}^{(j)}(r, \theta). \quad (1.19)$$

According to the metric form for the axial symmetry in the linear approximation via β parameter we introduce the notations describing explicitly the non perturbed (spherically symmetric case noted with upper index (0)) and perturbed terms (corresponding to $j = 1, 2$) in the metric,

$$\begin{aligned} e^{-\lambda(r, \theta)} &= e^{-\lambda^{(0)}(r)} [1 + \beta f(r, \theta)] + O(\beta^2), \\ e^{\nu(r, \theta)} &= e^{\nu^{(0)}(r)} [1 + \beta \Phi(r, \theta)] + O(\beta^2), \\ e^{\mu(r, \theta)} &= r^2 [1 + \beta U(r, \theta)] + O(\beta^2), \end{aligned} \quad (1.20)$$

and for the frame dragging frequency ω the odd orders

$$\omega(r, \theta) = \sqrt{\beta} q(r, \theta) + O((\sqrt{\beta})^3). \quad (1.21)$$

In the same way one performs a velocity expansion of the energy-momentum tensor, the pressure and energy density distributions, and of the kinetic energy,

$$P(r, \theta) = P^{(0)}(r) + \beta P^{(2)}(r, \theta) + O(\beta^2), \quad (1.22)$$

$$\varepsilon(r, \theta) = \varepsilon^{(0)}(r) + \beta \varepsilon^{(2)}(r, \theta) + O(\beta^2), \quad (1.23)$$

where $P^{(0)}$ and $\varepsilon^{(0)}$ denote the zero-order coefficients which correspond to non-deformed spherically symmetric stars.

Because of rotational symmetry the diagonal elements $g_{\mu\mu}^{(j)}(r, \theta)$ (no summation over μ) of the metric coefficients can be written as (j and l are even values only)

$$g_{\mu\mu}^{(j)}(r, \theta) = \sum_{l=0}^j (g_{\mu\mu})_l(r) P_l(\cos \theta). \quad (1.24)$$

The same is true also for the non diagonal elements, but the angular dependence is different (j and l values are now odd only). The case for the non diagonal term will be investigated in section 1.3.1, where the moment of inertia will be discussed.

In the case of a deformed distribution of the matter, the external metric has the form of the Kerr metric. However this solution is for black holes and does not correspond to a realistic stellar models. Therefore the external as well the internal solutions of the field and matter distributions can only be obtained either via a perturbation approximation or via a completely numerical treatment.

1.2.4 Static spherically symmetric star models

As a first step in the perturbation approach of a slowly rotating star one needs to find the internal gravitational field, the mass and matter distributions, the total gravitational mass, the radius and all other characteristic properties (including the metric functions) of spherically symmetric stars. The solution for the metric functions in empty space (i.e., the external solutions) are given by the Schwarzschild solution.

$$\begin{aligned}\lambda^{(0)}(r) &= -\ln[1 - 2GM/r], \\ \nu^{(0)}(r) &= -\lambda^{(0)}(r).\end{aligned}\tag{1.25}$$

where M is a constant of integration, which asymptotically is the Newtonian gravitational mass of the object.

These nonlinear equations, however, could be written in an elegant form suggested by Tolman, Oppenheimer and Volkoff, which are known as the TOV equations (Tolman, 1939; Oppenheimer and Volkoff, 1939), and solved in a way such that the internal solution matches the analytic external Schwarzschild solution. The TOV equation is given by (for a derivation, see, e.g., the textbook by Misner *et al.* (1973))

$$\frac{dP^{(0)}(r)}{dr} = -G[P^{(0)}(r) + \varepsilon^{(0)}(r)] \frac{m(r) + 4\pi P^{(0)}(r)r^3}{r[r - 2Gm(r)]}, \tag{1.26}$$

where $P^{(0)}$ and $\varepsilon^{(0)}$ denote the equation of state (EoS) describing the stellar matter. The quantity $m(r)$, defined as

$$m(r) = 4\pi \int_0^r \varepsilon^{(0)}(r')r'^2 dr', \tag{1.27}$$

stands for the amount of gravitational mass contained inside a sphere of radius r , with r denoting the distance from the center of the star. The star's total gravitational mass, M , is then given

$$M = m(R) = 4\pi \int_0^R \varepsilon^{(0)}(r')r'^2 dr', \tag{1.28}$$

where R denotes the radius of the star defined by $P(r = R) = 0$. Physically, the TOV equation describes the balance of gravitational and internal pressure forces at each radial distance inside the star. Both forces exactly cancel each other inside a static stellar configuration, as described by the TOV equation.

The TOV equation is solved numerically, for a given model for the EoS, by choosing a value for the star's central density and then integrating

Eq. (1.26) out to a radial location where the pressure becomes zero. So for any fixed choice of the EoS, the stars form a one-parameter sequence (parameter $\varepsilon_c^{(0)}$). An entire family of compact stars is obtained by solving the TOV equation for a range of central densities which result in the mass-radius relationship of compact stars. It is characterized by the existence of a maximum mass star (several maximum mass stars if permitted by the model chosen for the EoS). The stars are stable against gravitational collapse if they are on the stellar branch for which $\partial M/\partial\varepsilon_c^{(0)} > 0$. Stars on the stellar branch where $\partial M/\partial\varepsilon_c^{(0)} < 0$ are unstable against radial oscillations and will therefore not exist stably in the universe.

Each stellar model has unique solutions for $m(r)$, $P^{(0)}(r)$ and $\varepsilon^{(0)}(r)$ in terms of which the internal gravitational field (the metric coefficients) is defined as

$$\lambda^{(0)}(r) = -\ln[1 - 2Gm(r)/r], \quad (1.29)$$

$$\nu^{(0)}(r) = -\lambda^{(0)}(R_0) - 2G \int_r^{R_0} \frac{m(r') + 4\pi P^{(0)}(r')r'^3}{r'[r' - 2Gm(r')]} dr'. \quad (1.30)$$

The internal field solutions are smoothly connected to the external field solutions at the stellar surface, $r = R$. Once the internal pressure profiles are derived from the solution of the TOV equations, it is possible to compute other astrophysical quantities like baryonic mass, and also make the next step in the perturbation approach to define the moment of inertia and tidal deformabilities, which are of very great observational interest.

Of particular interest for astrophysical scenarios (stellar evolution) is the expression for the total baryon mass

$$\frac{dN_B(r)}{dr} = 4\pi r^2 \left(1 - \frac{2Gm(r)}{r}\right)^{-1/2} n(r), \quad (1.31)$$

where $n(r)$ is the baryon number density and $N_B(R)$ is the total baryon number of the star. This number is a characteristic conserved quantity and is very important in discussions of evolutionary scenarios of compact stars, see, e.g., Bejger *et al.* (2017); Ayvazyan *et al.* (2013); Chubarian *et al.* (2000); Poghosyan *et al.* (2001). The functions of the spherically symmetric solution in Eqs. (1.20) and (1.22) can be found from Eq. (1.5) and Eq. (1.9) in zeroth order of the Ω -expansion.

1.3 Tidal deformability of compact stars

The tidal deformability (TD) is a measure of the shape deformation property of the astrophysical object under the gravitational influence of another

nearby object. To determine it in the first order we need to consider a modification of the space-time metric when the distribution of matter of the star becomes elliptic. According to the symmetries of the metric coefficients introduced in Eq. (1.3) we have even orders $j = 0, 2, \dots$ for the diagonal elements¹. The the first correction corresponding to small deformations (small values of β) one can consider terms linear in β or equivalently the $j = 2$ perturbation approximation to the spherically symmetric star. We introduce some new notation and work under the assumption that $f_2(r) = -\Phi_2(r) = A(r)$ like in the expansion of the external solution, since $\nu^{(0)}(r) = -\lambda^{(0)}(r)$.

The non diagonal term could be taken to be zero, because we consider only the static case $q(r, \theta) = 0$ (the parameter defining the static deformation $\sqrt{\beta}$ does not change the sign under time reversal $t \rightarrow -t$) and $U_2(r) = K(r)$, so that we have

$$\begin{aligned} ds^2 = & e^{\lambda^{(0)}(r)} [1 + \beta A(r) P_2(\theta)] dt^2 \\ & - e^{\nu^{(0)}(r)} [1 - \beta A(r) P_2(\theta)] dr^2 \\ & - r^2 [1 - \beta K(r) P_2(\theta)] (d\theta^2 + \sin^2 \theta d\varphi^2) . \end{aligned} \quad (1.32)$$

In this approximation, without loss of generality, one can set the values of $f_0 = \Phi_0 = U_0 = 0$, because we neglect the contribution of the deformation energy to the gravitational mass. The equations show that $K'(r) = A'(r) + \nu^{(0)'}(r)A(r)$ the prime symbol denoting the derivative of those quantities with respect to r . The functions $A(r)$ and $B(r) = dA/dr$ obey the differential equations

$$\begin{aligned} \frac{dA(r)}{dr} &= B(r); \quad (1.33) \\ \frac{dB(r)}{dr} &= 2 \left(1 - 2G \frac{m(r)}{r} \right)^{-1} \\ &\times A(r) \left\{ -2\pi \left[5\varepsilon^{(0)}(r) + 9P^{(0)}(r) + \frac{1}{c_s^2} \left(\varepsilon^{(0)}(r) + P^{(0)}(r) \right) \right] \right. \\ &+ \frac{3}{r^2} + 2 \left(1 - 2G \frac{m(r)}{r} \right)^{-1} \left[G \left(\frac{m(r)}{r^2} + 4\pi r P^{(0)}(r) \right) \right]^2 \left. \right\} \\ &+ \frac{2B(r)}{r} \left(1 - 2G \frac{m(r)}{r} \right)^{-1} \\ &\times \left\{ -1 + G \left[\frac{m(r)}{r} + 2\pi r^2 \left(\varepsilon^{(0)}(r) - P^{(0)}(r) \right) \right] \right\}. \end{aligned} \quad (1.34)$$

¹Notation corresponds to the work of Chubarian *et al.* (2000).

Here, $c_s^2 = dP/d\varepsilon$ is the square of the speed of sound, which is equivalent to the knowledge of the equation of state. The pressure profile provided by solving the TOV equations will complement the above equations.

The system is to be integrated with the asymptotic behavior of metric functions $A(r) = a_0 r^2$ and $B(r) = 2a_0 r$ as $r \rightarrow 0$, The a_0 is a constant that quantifies the deformation of the star which can be taken arbitrary. This constant corresponds to the choice of β as an external parameter. Since it cancels in the expression for the Love number and in all other quantities in consideration its value is not important. Using the solution on the surface at $r = R$ and the following combination

$$y = \frac{RB(R)}{A(R)}, \quad (1.35)$$

it is possible to compute the $l = 2$ Love number (Hinderer, 2008; Damour and Nagar, 2009; Binnington and Poisson, 2009; Yagi and Yunes, 2013; Hinderer *et al.*, 2010):

$$\begin{aligned} k_2 = & \frac{8C^5}{5}(1-2C)^2[2+2C(y-1)-y] \\ & \times \left\{ 2C[6-3y+3C(5y-8)] \right. \\ & + 4C^3[13-11y+C(3y-2)+2C^2(1+y)] \\ & \left. + 3(1-2C)^2[2-y+2C(y-1)]\ln(1-2C) \right\}^{-1}, \end{aligned}$$

where M/R in the expression $C = GM/R$ is the compactness of the star ($2C$ is the ratio of gravitational radius to spherical radius).

The dimensionless tidal deformability parameter is defined as $\Lambda = \lambda/M^5$, a quantity defined for small tidal deformabilities. Here λ is the TD of the star with a gravitational mass M , just as defined above. In addition, the love number is related to TD and defined as

$$k_2 = \frac{3}{2}\lambda R^{-5}. \quad (1.36)$$

In the investigations and observations of the process of neutron star merging the TD Λ is a key parameter characterising the stiffness of equation of state of the stellar matter.

1.3.1 Moment of inertia

The moment of inertia is one of the main characteristics of the mechanical properties of the rotating body, therefore one needs to define it also for the

relativistic objects as neutron star obeying the gravitational field contribution to the rotational motion. The baryonic mass is an important quantity often associated with explosive events, where it can be conserved while the gravitational mass of the star suffers modifications (Alvarez-Castillo *et al.*, 2015; Bejger *et al.*, 2017). The moment of inertia is related to the *glitch* phenomenon, which is a sudden spin-up in the general spin-down evolution of rotation frequencies, observed for some pulsars, see (Haskell and Melatos, 2015) and references therein. Moreover, it is expected to be measured in pulsar binaries, providing a strong constraint on the compact star EoS (Lattimer and Prakash, 2007).

In a very simplified way one can estimate the impact of relativistic effects on the moment of inertia from (Ravenhall and Pethick, 1994)

$$I \simeq \frac{C_J}{1 + 2GJ/R^3}, \quad (1.37)$$

where J denotes the total, conserved angular momentum. The quantity C_J is given by

$$C_J = \frac{8\pi}{3} \int_0^R r^4 \left(\varepsilon^{(0)}(r) + P^{(0)}(r) \right) \frac{1}{1 - 2Gm(r)/r} dr, \quad (1.38)$$

which can be readily computed since only the knowledge of spherically symmetric quantities is required, which are easy to compute.

However, because of the deformation of the star due to rotation and the impact of the gravitational field on the rotational inertia of the star, the moment of inertia becomes a function of the rotational state, i.e., a function of the angular velocity or spin frequency of the neutron star. To take all these effects into account in the defining expression for the moment of inertia we will follow the steps of our perturbation approach.

By definition, the angular momentum of the star in the case of stationary rotation is a conserved quantity and can be expressed in invariant form

$$J = \int T_{\phi}^t \sqrt{-g} dV, \quad (1.39)$$

where $\sqrt{-g}dV$ is the invariant volume and $g = \det ||g_{\mu\nu}||$. For the case of slow rotation where the shape deformation of the rotating star can be neglected and using the definition of the moment of inertia $I_0(r) = J_0(r)/\Omega$ accumulated in the sphere with radius r , we obtain from Eq. (1.39)

$$\frac{dI_0(r)}{dr} = \frac{8\pi}{3} r^4 [\varepsilon^{(0)}(r) + P^{(0)}(r)] e^{(-\nu^{(0)}(r) + \lambda^{(0)}(r))/2} \frac{\bar{\omega}(r)}{\Omega}.$$

Here $\bar{\omega}$ the difference of the frame dragging frequency $-\omega$ and the angular velocity Ω . In general relativity, due to the Lense-Thirring law, rotational effects are described by

$$\bar{\omega} \equiv \Omega + \omega(r, \theta). \quad (1.40)$$

This expression is approximated from the exact expression of the energy momentum tensor coefficient T_ϕ^t and the metric tensor in the axial symmetric case.

We keep only two non-vanishing components of the 4-velocity

$$\begin{aligned} u^\phi &= \Omega u^t, \\ u^t &= 1/\sqrt{e^\nu - r^2 e^\mu \bar{\omega}^2 \sin^2 \theta}. \end{aligned} \quad (1.41)$$

because we assume that the star due to high viscosity (ignoring the superfluid component of the matter) rotates stationary as a solid body with an angular velocity Ω that is independent of the spatial coordinates. The time scales for changes in the angular velocity which we will consider in our applications are well separated from the relaxation times at which hydrodynamical equilibrium is established, so that the assumption of a rigid rotator model is justified.

Now besides of central energy density $\varepsilon(0)$ of the star configuration the angular velocity of the rotation Ω is an additional parameter of the theory.

As a next step, going beyond the spherically symmetric case that corresponds to the first-order approximation, we solve Eq. (1.8), where the unknown function is $q(r, \theta)$ which is defined by Eq. (1.21) and scaled such that it is independent of the angular velocity. Using the static solutions Eqs. (1.26) and (1.29), and the representation of $q(r, \theta)$ by the series of the Legendre polynomials,

$$q(r, \theta) = \sum_{m=0}^{\infty} q_m(r) \frac{dP_{m+1}(\cos \theta)}{d \cos \theta}, \quad (1.42)$$

one can see that this series is truncated and only the coefficient $q_0(r)$ is nontrivial, i.e., $q_m(r) = 0$ for $m > 0$, see (Hartle, 1967; Chubarian *et al.*, 2000). Therefore one can write down the equations for $\bar{\omega}(r) = \Omega(1 + q_0(r)/\Omega_0)$, which is more suitable for the solution of the resulting equation in first order

$$\frac{1}{r^4} \frac{d}{dr} \left[r^4 j(r) \frac{d\bar{\omega}(r)}{dr} \right] + \frac{4}{r} \frac{dj(r)}{dr} \bar{\omega}(r) = 0, \quad (1.43)$$

which corresponds to Ref. (Hartle, 1967), where it was obtained using a different representation of the metric. In this equation we use the notation

$j(r) \equiv e^{-(\nu^{(0)}(r)+\lambda^{(0)}(r))/2}$, where $j(r) = 1$ for $r > R_0$, i.e., outside of stellar configuration.

Using this equation one can reduce the second order differential equation (1.43) to the first order one

$$\frac{d\bar{\omega}(r)}{dr} = \frac{6GJ_0(r)}{r^4 j(r)}. \quad (1.44)$$

and solve (1.43) as a coupled set of first order differential equations, one for the moment of inertia (1.39) and the other (1.44) for the frame dragging frequency $\bar{\omega}(r)$.

This system of equations is valid inside and outside the matter distribution. In the center of the configuration $I_0(0) = 0$ and $\bar{\omega}(0) = \bar{\omega}_0$. The finite value $\bar{\omega}_0$ has to be defined such that the dragging frequency $\bar{\omega}(r)$ smoothly joins the outer solution

$$\bar{\omega}(r) = \Omega \left(1 - \frac{2GI_0}{r^3} \right). \quad (1.45)$$

at $r = R_0$, and approaches Ω in the limit $r \rightarrow \infty$. In the external solution (1.45) the constant $I_0 = I_0(R_0)$ is the total moment of inertia of the slowly rotating star and $J_0 = I_0\Omega$ is the corresponding angular momentum. In this order of approximation, I_0 is a function of the central energy density or the total baryon number only. This solution remains connected to the spherically distributed matter and therefore does not differ too much from our previous expression, which uses this solution to incorporate the relativistic corrections.

However, to find the explicit dependence of the moment of inertia on the angular velocity, one needs to take the second step and account for the deformation of the stellar configuration, which, in the framework of our scheme, is a second-order correction.

1.3.2 Rotational deformation and moment of inertia

To calculate these contributions and the internal structure of the rotating star which is deformed due to centrifugal force one needs to return to our perturbation description and take into the corrections in the diagonal elements of the metric and the energy-momentum tensor, as in the equations above with the parameter $\beta = (\Omega/\Omega_0)^2$.

For a more detailed description of the solutions of the field equations in the $\sim O(\Omega^2)$ approximation we refer to the works of Hartle (1967) as well as Chubarian *et al.* (2000). Since these equations have a complicated form,

here we will discuss only the qualitative meaning of the physical quantities concerning the star's deformation and its moment of inertia.

In Ω^2 -approximation the shape of the star is an ellipsoid, and each of the equal-pressure (isobar) surfaces in the star is an ellipsoid as well. All diagonal elements of the metric and energy-momentum tensors could be represented as a series expansion in Legendre polynomials, as we have already discussed in the previous section where it has been noted that the only non vanishing solutions obeying the continuity conditions on the surface with the external solution of fields are those with $l = 0, 2$.

The deformation of the isobaric surfaces can be parameterised by the deformation shifts $R(r, \theta) - r = \Delta(r, \theta)$ from the spherical shape. It describes the deviation from the spherical distribution as a function of radius r for a fixed polar angle θ and is completely determined by

$$R(r, \theta) = r + \left(\frac{\Omega}{\Omega_0} \right)^2 [\Delta_0(r) + \Delta_2(r)P_2(\cos \theta)], \quad (1.46)$$

since the expansion coefficients of the deformation $\Delta_l(r)$ are connected with the pressure corrections

$$\Delta_l(r) = -\frac{p^{(l)}(r)}{dP^{(0)}(r)/dr}. \quad (1.47)$$

$l \in \{0, 2\}$ is the polynomial index in the angular expansion in Legendre polynomials, analogous to Eq. (1.24). The function $R(R_0, \theta)$ is the radius where $p(R(R_0, \theta)) = 0$. To avoid confusion, we denote the spherical radius as R_0 , which is not anymore the actual radius, but rather $R(R_0, \theta)$ which is the distance of the stellar surface from the center of the configuration at a polar angle θ . In particular, we define the equatorial radius as $R_e = R(R_0, \theta = \pi/2)$, the polar radius as $R_p = R(R_0, \theta = 0)$, and the eccentricity as $\epsilon = \sqrt{1 - (R_p/R_e)^2}$, all three quantities characterizing the deformed shape of the star.

Using this the same approach we write the correction to the moment of inertia as $\Delta I(r) = I(r) - I_0(r)$ and represent it as a sum of several different contributions,

$$\Delta I = \Delta I_{\text{Redist.}} + \Delta I_{\text{Shape}} + \Delta I_{\text{Field}} + \Delta I_{\text{Rotation}}. \quad (1.48)$$

Since these contributions are obtained from the exact expression of angular momentum in the integral form the first three contributions can also be expressed by integrals of the form

$$\Delta I_\alpha = \int_0^{I_0(R_0)} dI_0(r) [W_0^{(\alpha)}(r) - W_2^{(\alpha)}(r)/5], \quad (1.49)$$

where integration is taken from the angular averaged modifications of the matter distribution, the shape of the configuration and the gravitational fields,

$$W_l^{(\text{Field})}(r) = \left(\frac{\Omega}{\Omega_0} \right)^2 \{2U_l(r) - [f_l(r) + \Phi_l(r)]/2\}, \quad (1.50)$$

$$W_l^{(\text{Shape})}(r) = \left(\frac{\Omega}{\Omega_0} \right)^2 \frac{d \Delta_l(r)}{dr}, \quad (1.51)$$

$$W_l^{(\text{Redist.})}(r) = \left(\frac{\Omega}{\Omega_0} \right)^2 \frac{p_l(r) + \varepsilon_l(r)}{p^{(0)}(r) + \varepsilon^{(0)}(r)}, \quad (1.52)$$

respectively. All quantities appearing have been determined from the Eq. (1.5) in second order approximation. The contribution of the change of the rotational energy to the moment of inertia is given by

$$\Delta I_{\text{Rotation}} = \frac{4}{5} \int_0^{I_0(R_0)} dI_0(r) \left[r^2 \bar{\omega}^2(r) e^{-\nu_0(r)} \right]. \quad (1.53)$$

and includes the frame dragging contribution.

In the next sections of this chapter we will discuss results for the moment of inertia along with stability conditions. We note that a consistent discussion of the stability of rotating stars requires one to take into account the contribution of the rotational energy to the mass energy, as well as the corresponding corrections to the moment of inertia.

1.4 Models for the EoS with a strong phase transition

In this contribution, we focus on EoS models which describe a strong phase transition in the sense that upon solving the TOV equations with them compact star sequences are obtained which exhibit a third family branch in the mass-radius or mass-central (energy) density diagram which is separated from the second family of neutron stars by a sequence of unstable configurations. The possibility of the very existence of a third family of compact stars as a consequence of a strong phase transition in dense nuclear matter, together with a sufficient stiffening of the high-density matter that can be expressed by a strong increase in the speed of sound (but not violating the causality bound) has been discussed by Gerlach as early as 1968 [Gerlach (1968)]. Let us note here that the very existence of such a third family of compact stars is an effect of strong, general relativistic gravity! Namely, that the compactification which accompanies the strong phase transition of the star leads to a reduction of the gravitational mass

of the hybrid star configuration from which it only recovers (and thus escapes gravitational collapse) when after the transition the hybrid star core consists of sufficiently stiff high-density matter.

Such EoS lead to mass-radius relationships for hybrid stars that have been classified (D)isconnected or (B)oth in Ref. [Alford *et al.* (2013)]. The "D" topology consists of a hadronic and a hybrid star branch, both of which being gravitationally disconnected from each other. In contrast to this, the "B" topology consists of a branch of stable hadronic stars followed by stable hybrid stars, which are gravitationally disconnected from a second branch of stable hybrid stars. For the introduction of this classification scheme, the constant-speed-of-sound (CSS) EoS was used in [Alford *et al.* (2013)] for describing the high-density matter, see also Ref. [Zdunik and Haensel (2013)] for the justification of its validity in the case of color superconducting quark matter EoS. The first demonstration that high-mass twin stars and thus a corresponding high-mass third family sequence with $M_{\max} > 2 M_{\odot}$ were possible, has been given in [Alvarez-Castillo and Blaschke (2013)] The intricacy of an equation of state describing a third family of stars (with twin stars at high or low masses as a consequence) consists in the fact that one needs, on the one hand, a sufficiently large jump in energy density $\Delta\varepsilon$ and a relatively low critical energy density ε_c at the transition point to fulfil the Seidov criterion (1.1) for gravitational instability (i.e., a stiff nuclear matter EoS has to be followed by a soft high-density one), while on the other the high-density EoS needs to become sufficiently stiff directly after the phase transition, without violating the causality condition ($c_s^2 < 1$). With the CSS parametrization, these constraints could be fulfilled relatively straightforwardly by dialling $c_s^2 = 1$ and adjusting a sufficiently large value of $\Delta\varepsilon$ by hand.

The question arose whether a hybrid star EoS describing a third family of compact stars with a maximum mass above $2 M_{\odot}$ could also be obtained when applying the standard scheme of a two-phase approach based on a realistic nuclear matter EoS and a microscopically well-founded quark matter EoS, both joined, e.g., by a Maxwell construction. A positive answer was given already in 2013, when two examples of this kind were presented in [Blaschke *et al.* (2013a)], where the excluded-volume corrected nuclear EoS APR and DD2 were joined with a quark matter EoS based on the nonlocal NJL model approach [Blaschke *et al.* (2007); Benic *et al.* (2014)], augmented with a density dependent repulsive vector meanfield that was constructed by employing a thermodynamically consistent interpolation scheme introduced in Ref. [Blaschke *et al.* (2013b)]. Such an interpolation scheme, based on the

nonlocal, color superconducting NJL model of [Blaschke *et al.* (2007)], but extended to address also a density-dependent bag-pressure that facilitates a softening of the quark matter EoS in the vicinity of the deconfinement transition, has recently been developed in [Alvarez-Castillo *et al.* (2019)], guided by a relativistic density functional (RDF) approach to quark matter [Kaltenborn *et al.* (2017)] with an effective confinement mechanism according to the string-flip model [Horowitz *et al.* (1985); Ropke *et al.* (1986)]. This approach has been applied very successfully to describe a whole class of hybrid EoS with a third family branch fulfilling the modern compact star constraints [Ayriyan *et al.* (2018); Alvarez-Castillo *et al.* (2019)]. In the RDF approach to the string-flip model of quark matter an essential element is the ansatz for the nonlinear density functional resembling confinement and embodying the aspect of in-medium screening of the string-type confining interaction within an excluded volume mechanism. Another nonlinearity term in the density functional embodies the stiffening of quark matter at high densities in a similar way as it was obtained from 8-quark interactions in the NJL model [Benic (2014)] that were an essential part of the description of high-mass twins in [Benic *et al.* (2015)]. Both nonlinearities, due to (de)confinement and high-density stiffening, are mimicked in a rather flexible way by the twofold interpolation scheme suggested in [Alvarez-Castillo *et al.* (2019)] which can be reinterpreted as a generalization of the nonlocal NJL model with chemical-potential-dependent parameters.

Having discussed the successful approaches to construct EoS with a strong phase transition which account for third family branches of compact stars and can be recognized observationally by the mass twin phenomenon, we would like to mention which ingredients are indispensable for obtaining this feature and which approaches have failed to obtain it. An excellent illustration of the various possibilities to join by interpolation hadronic and quark matter phases which themselves have different characteristics of stiffness, can be found in the recent review of Ref. [Baym *et al.* (2018)]. However, despite being quite general, the case of the third family branch and mass-twin compact stars could not be captured! The reason can be found elucidated in Ref. [Alvarez-Castillo *et al.* (2019)], where it is demonstrated for a representative set of hadronic as well as quark matter EoS of varying degree of stiffness, that either a phase transition in the relevant domain of densities is entirely absent or results in a hybrid star branch that is directly connected to the hadronic branch which therefore does not form a third family of stars. The generated patterns are very similar to the results of Ref. [Orsaria *et al.* (2014)] which also uses the nonlocal NJL

model for describing the quark phase of matter. The clue to obtaining third family sequences within microscopically motivated studies is a subtle softening followed by a stiffening of quark matter that can be realized employing the thermodynamically consistent interpolation procedure between different parametrizations of the same quark EoS (e.g., varying the vector meson coupling strength) before applying a Maxwell-, Gibbs-, or pasta phase transition construction.

We have described here the state-of-the-art modeling of EoS with a strong phase transition that are based on microscopic models of high-density (quark) matter. Besides these, there is a large number of simple EoS parametrizations that are also in use for discussing third family sequences fulfilling the constraint of a high maximum mass of the order of $2 M_{\odot}$. These are basically the classes of CSS based models and multi-polytrope approaches. Without attempting completeness, we would like to mention Refs. [Alford *et al.* (2015); Alford and Han (2016); Christian *et al.* (2018); Alford and Sedrakian (2017); Paschalidis *et al.* (2018); Christian *et al.* (2019); Montana *et al.* (2019); Han and Steiner (2019)] from the class of CSS models. A particularly interesting work is the extension by Alford and Sedrakian [Alford and Sedrakian (2017)], who demonstrated that also a fourth family of hybrid stars can be obtained and besides mass-twins there are also mass-triples possible. The multi-polytrope EoS have been a workhorse for numerical relativity studies of astrophysical scenarios since many years. The approach to constrain the multi-polytrope parameters from observations of masses and radii as introduced by Read *et al.* [Read *et al.* (2009)] has then been developed further with great resonance in the community by Hebeler *et al.* (2010, 2013). While in Read *et al.* (2009) one already finds a one parameter set describing high-mass twin stars that have not yet become a matter of interest in the community, the third family branch in the multi-polytrope approaches has been mainly overlooked (see, e.g., Raithel *et al.* (2016); Miller *et al.* (2019)), but was digged up in Ref. [Alvarez-Castillo and Blaschke (2017)] where it was found that one should have at least a four-polytrope ansatz and suitably chosen densities for the matching of the polytrope pieces of the EoS, see also Annala *et al.* (2018); Paschalidis *et al.* (2018); Hanauske *et al.* (2018).

An important issue when discussing strong first-order phase transitions is the appearance of structures of finite size, like bubbles and droplets in the boiling/condensation transitions of the water-vapour transformations. In general, different shapes in the new phase are possible like spherical, cylindrical and planar structures, which have been dubbed "pasta structures".

Their size and thermodynamical favorability depends on the surface tension between the subphases and the effects of the Coulomb interaction, including screening. The resulting pressure in the mixed phase is then no longer constant as in the Maxwell construction case, but also not as dramatically changing when the surface tension is neglected [Glendenning (1992)]. For details concerning the quark-hadron transition pasta phases under neutron star constraints see, e.g., Refs. [Na *et al.* (2012); Yasutake *et al.* (2014); M. Spinella *et al.* (2016)]. It is interesting to note that a simple one-parametric parabolic approximation of the pressure versus chemical potential dependence can give a satisfactory agreement with a full pasta phase calculation and that the single parameter can be directly related to the surface tension [Maslov *et al.* (2018)]. It could be demonstrated that the third family feature of an EoS with strong phase transition is rather robust against pasta phase effects, see Ayriyan *et al.* (2018).

In the present work, we will use the multi-polytrope approach to the EoS describing a third family of compact stars and also discuss the effect of mimicking the pasta structures in the mixed phase by a polynomial interpolation. The results shall not depend qualitatively on these simplifying assumptions but be of rather general nature and also applicable to more realistic types of EoS as discussed above.

1.4.1 Multi-polytrope approach to the EoS

In this section we present an EoS model that features a strong first-order phase transition from hadron to quark matter. They are labeled “ACB” following (Paschalidis *et al.*, 2018) and consist of a piecewise polytropic representation (Read *et al.*, 2009; Hebeler *et al.*, 2013; Raithel *et al.*, 2016) of the EoS at supersaturation densities ($n_1 < n < n_5 \gg n_0$):

$$P(n) = \kappa_i (n/n_0)^{\Gamma_i}, \quad n_i < n < n_{i+1}, \quad i = 1 \dots 4, \quad (1.54)$$

where Γ_i is the polytropic index in each of the density regions labeled by $i = 1 \dots 4$. We fix Γ_1 such that a stiff nucleonic EoS provided in (Hebeler *et al.*, 2013) can be described. The second polytrope shall correspond to a first-order phase transition therefore in this region the pressure must be constant, given by $P_c = \kappa_2 (\Gamma_2 = 0)$. The remaining polytropes, in regions 3 and 4, that lie above the phase transition shall correspond to high-density matter, like stiff quark matter.

In order to compute the remaining thermodynamic variables of the EoS,

we utilize the formulae given in the Appendix of Ref. (Zdunik *et al.*, 2006),

$$P(n) = n^2 \frac{d(\varepsilon(n)/n)}{dn}, \quad (1.55)$$

$$\varepsilon(n)/n = \int dn \frac{P(n)}{n^2} = \frac{1}{n_0^{\Gamma_i}} \int dn \kappa n^{\Gamma_i-2} = \frac{1}{n_0^{\Gamma_i}} \frac{\kappa n^{\Gamma_i-1}}{\Gamma_i-1} + C, \quad (1.56)$$

$$\mu(n) = \frac{P(n) + \varepsilon(n)}{n} = \frac{1}{n_0^{\Gamma_i}} \frac{\kappa \Gamma_i}{\Gamma_i-1} n^{\Gamma_i-1} + m_0, \quad (1.57)$$

where we fix the integration constant C by the condition that $\varepsilon(n \rightarrow 0) = m_0 n$. Now we can invert the above expressions to obtain

$$n(\mu) = \left[n_0^{\Gamma_i} (\mu - m_0) \frac{\Gamma_i - 1}{\kappa \Gamma_i} \right]^{1/(\Gamma_i-1)}, \quad (1.58)$$

so that the chemical potential dependent pressure for the polytrope EoS (1.54) can be written as

$$P(\mu) = \kappa \left[n_0^{\Gamma_i} (\mu - m_0) \frac{\Gamma_i - 1}{\kappa \Gamma_i} \right]^{\Gamma_i/(\Gamma_i-1)}. \quad (1.59)$$

The above form of the pressure (1.59) is suitable to perform a Maxwell construction of a first-order phase transition between the hadron and quark phases. The model parameters for the mass twin cases that we consider in this work are given in table 1.3.

Table 1.3 EOS models ACB4 and ACB5 (Paschalidis *et al.*, 2018). The parameters are defined in Eq. (1.54) in the main text. The first polytrope ($i = 1$) describes the nuclear EoS at supersaturation densities, the second polytrope ($i = 2$) corresponds to a first-order phase transition with a constant pressure P_c for densities between n_2 and n_3 . The remaining polytropes lie in regions 3 and 4, i.e., above the phase transition and correspond to high-density matter, e.g., quark matter. The last column shows the maximum masses M_{\max} on the hadronic (hybrid) branch corresponding to region 1 (4). The minimal mass M_{\min} on the hybrid branch is shown for region 3.

ACB	i	Γ_i	κ_i [MeV/fm ³]	n_i [1/fm ³]	$m_{0,i}$ [MeV]	$M_{\max/\min}$ [M_{\odot}]
4	1	4.921	2.1680	0.1650	939.56	2.01
	2	0.0	63.178	0.3174	939.56	–
	3	4.000	0.5075	0.5344	1031.2	1.96
	4	2.800	3.2401	0.7500	958.55	2.11
5	1	4.777	2.1986	0.1650	939.56	1.40
	2	0.0	33.969	0.2838	939.56	–
	3	4.000	0.4373	0.4750	995.03	1.39
	4	2.800	2.7919	0.7500	932.48	2.00

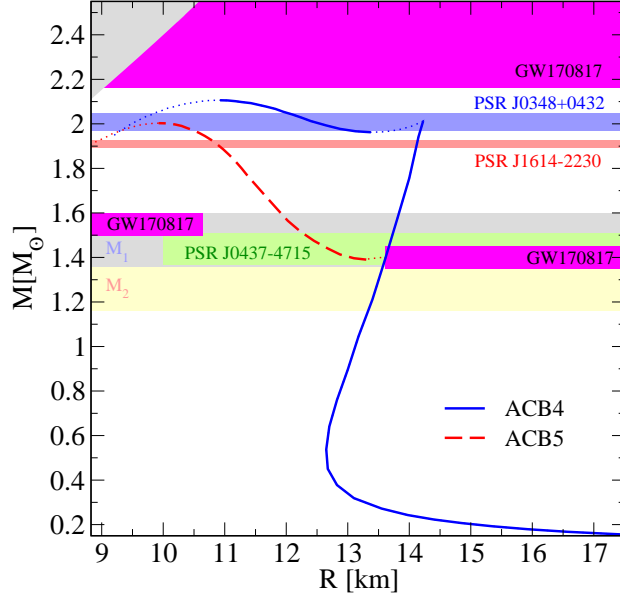


Fig. 1.1 Mass-radius relationship. The two curves correspond to the compact star sequences resulting after integration of the TOV equations for the ACB4 and ACB5 EoS. The blue, red and yellow regions correspond to mass measurements of the PSR J0348+0432, PSR J1614-2230 and PSR J0437-4715 pulsars, respectively. The latter is the target of the NICER detector that shall provide a measurement for its radius (Arzoumanian *et al.*, 2009). The areas labeled M1 and M2 correspond to the mass estimates of the compact stars that merged in the GW170817 event that was detected through gravitational radiation (Abbott *et al.*, 2017). The magenta marked areas labeled GW170817 are excluded by the GW170817 event (Bauswein *et al.*, 2017). An upper limit on the maximum mass of nonrotating compact stars of $2.16M_{\odot}$ has been estimated in [Rezzolla *et al.* (2018)]. The region excluded by this estimate is shown by the magenta area, too. This limit will be reconsidered again later in light of the material presented in this work. The grey area in the upper left corner corresponds to a forbidden region where causality is violated.

The ACB4 EoS features a first order phase transition at a rather high nucleon number density value, $n_2 = 0.3174 \text{ fm}^{-3}$ that produces an instability in a $2.0M_{\odot}$ neutron star, providing an example of the high-mass twins phenomenon. On the contrary, the ACB5 EoS presents a phase transition that occurs at the lower value of $n_2 = 0.284 \text{ fm}^{-3}$. In that case the instability occurs for stars with $1.4M_{\odot}$, providing a scenario for low-mass twin stars. This low density value for the phase transition of about two times

saturation density, is particularly feasible in neutron star matter, where the effect of the isospin asymmetry manifests in the so called asymmetry energy which stiffens the EoS with respect to the symmetric case, equal number of protons and neutrons in hadronic matter. Figure 1.1 shows the resulting mass-relation curves for these two EoS featuring mass twins together with measurements and constraints regions.

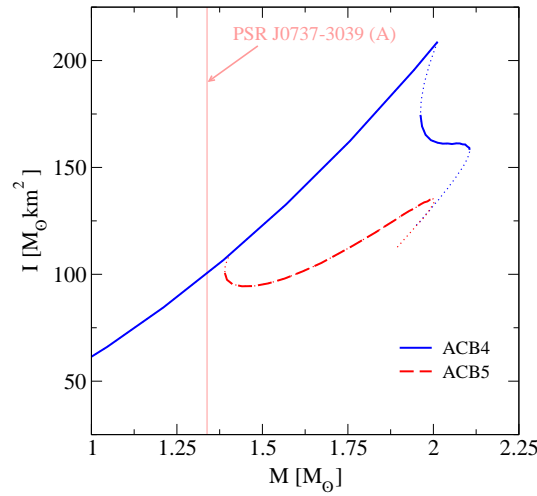


Fig. 1.2 Moment of inertia as a function of gravitational mass of the star for the two EoS cases ACB4 and ACB5. For an orientation, we indicate the precisely determined mass of the star PSR J0737-3039 (A), for which a measurement of the moment of inertia will become possible soon. This will provide further constraints on the EoS of dense matter and astrophysical scenarios involving compact stars.

1.4.2 EoS including mixed phase effects (pasta phases)

In this section we introduce a mixed phase approach to mimic pasta structures in regions of both the hadronic and quark EoS around the Maxwell critical point (μ_c, P_c) . The method used is the replacement interpolation method (RIM) (Abgaryan *et al.*, 2018) that consists of replacing the EoS in the aforementioned domain by a polynomial function:

$$P_M(\mu) = \sum_{q=1}^N \alpha_q (\mu - \mu_c)^q + (1 + \Delta_P) P_c, \quad (1.60)$$

with Δ_P as free parameter that adds pressure to the mixed phase at μ_c . Generally, all parametrizations of the type shown in Eq. (1.60) for the mixed phase pressure are even order ($N = 2k, k=1, 2, \dots$) polynomials which we refer to as G_k . In order to smoothly match the EoS at μ_H and μ_Q up to the k -th derivative of the pressure the following conditions shall be fulfilled

$$P_H(\mu_H) = P_M(\mu_H), \quad (1.61)$$

$$P_Q(\mu_Q) = P_M(\mu_Q), \quad (1.62)$$

$$\frac{\partial^k}{\partial \mu^k} P_H(\mu_H) = \frac{\partial^k}{\partial \mu^k} P_M(\mu_H), \quad (1.63)$$

$$\frac{\partial^k}{\partial \mu^k} P_Q(\mu_Q) = \frac{\partial^k}{\partial \mu^k} P_M(\mu_Q), \quad (1.64)$$

with α_q, μ_H and μ_Q being determined by the above system of equations.

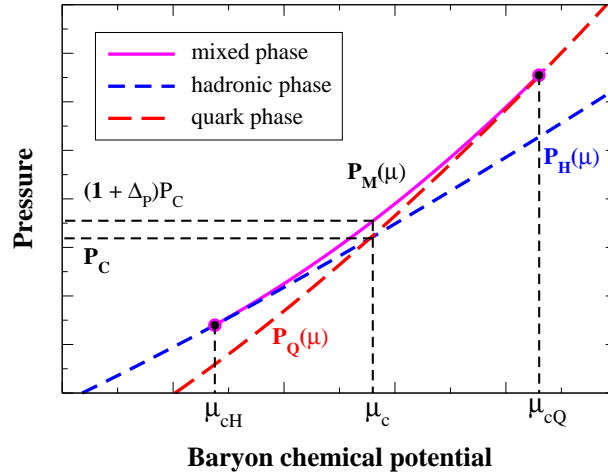


Fig. 1.3 Replacement interpolation function $P_M(\mu)$ obtained from the mixed phase constructions around the Maxwell construction. The resulting EoS connects the three points $P_H(\mu_H)$, $P_c + \Delta P = P_c(1 + \Delta_P)$, and $P_Q(\mu_Q)$. Figure taken from (Abgaryan *et al.*, 2018).

For the sake of simplicity we employ the parabolic model G_1 of the RIA as introduced in (Ayriyan and Grigorian, 2018; Ayriyan *et al.*, 2018):

$$P_M(\mu) = \alpha_2 (\mu - \mu_c)^2 + \alpha_1 (\mu - \mu_c) + (1 + \Delta_P) P_c, \quad (1.65)$$

where the parameters $\alpha_1, \alpha_2, \mu_H$ and μ_Q are to be determined as described above, from the continuity conditions at the Maxwell construction critical

point:

$$P_H(\mu_H) = P_M(\mu_H), \quad (1.66)$$

$$P_Q(\mu_Q) = P_M(\mu_Q), \quad (1.67)$$

$$n_H(\mu_H) = n_M(\mu_H), \quad (1.68)$$

$$n_Q(\mu_Q) = n_M(\mu_Q). \quad (1.69)$$

Figure 1.3 shows a schematic representation of the RIM method based on the Maxwell construction between the hadronic and quark EoS.

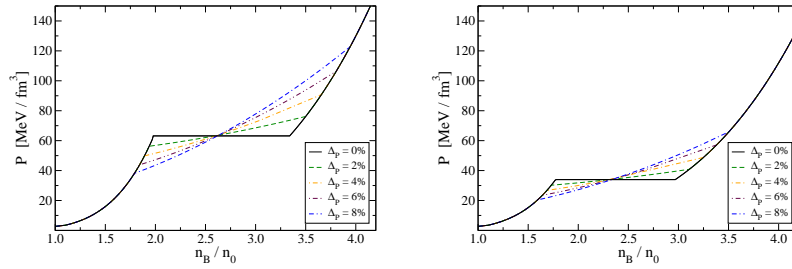


Fig. 1.4 Mixed phase mass twins equations of state for high mass NS onset (left) and low mass NS onset (right). The horizontal plateau at the phase transition corresponds to the Maxwell construction case. As the Δ_P parameter is increased successively, the plateau gives way to straight lines with increasing slope values.

In addition, figure 1.4 shows the mixed phase equations of state for both low and high mass twins. The effect of the mimicked geometrical structures is quantified by the Δ_P parameter. It is evident that the order of the G function will result in whether or not there are discontinuities for the derivatives of the P_M function. For instance, the square of the speed of sound, c_s^2 , is proportional to the second derivative of G with respect to μ , see figure 1.5.

The result is that G_1 presents a clear discontinuity in the speed of sound at ε_c and $\varepsilon_c + \Delta\varepsilon$, whereas in between i.e., in the latent heat region, the speed of sound slightly increases. On the contrary, the construction G_2 allows for a continuous speed of sound, however it is not smoothly connected at ε_c and $\varepsilon_c + \Delta\varepsilon$. Only G_3 is capable of joining smoothly the speed of sound between the hadron and quark EoS at the critical points.

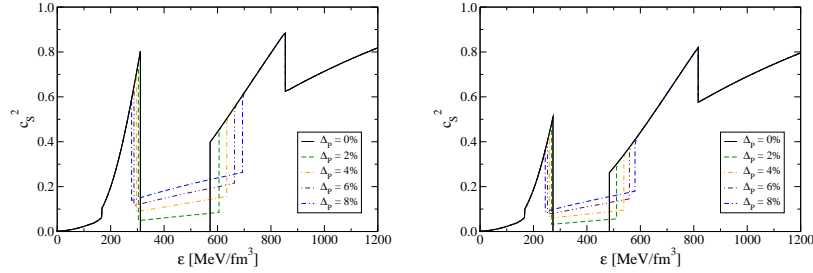


Fig. 1.5 Squared speed of sound as a function of the energy density for the mixed phase mass twins equations of state with high mass HS onset (ACB4, left panel) and low mass HS onset (ACB5, right panel).

1.5 Results

1.5.1 TOV solutions for mixed phase models

In figure 1.7 we show the results of the mass-radius diagram as a solution of the TOV equations for the equations of state ACB4 (left panel) which exhibits high mass twin stars and ACB5 (right panel) which describes low mass twins, depending on the value of the mixed phase parameter Δ_P . In the insets we give a magnified view on the region of the maximum mass of the hadronic branch of the sequence, where the dotted lines indicate the unstable solutions that qualify the corresponding EoS as one with a third family. We can read off to the accuracy of the given 1% steps what the critical value for Δ_P is when the disconnected second and third families would merge to a connected hybrid star sequence.

While for the case of ACB4 the variation of Δ_P does not affect the mass-radius diagram in the mass region of the compact star merger GW170817, the corresponding variation for ACB5 leads to strong effects in that mass region. We therefore consider the tidal deformability in both cases in the next subsection.

1.5.2 Tidal deformability predictions

Together with the solution of the TOV equations, one can solve for the dimensionless tidal deformability $\Lambda(M)$ for the given EoS. After that, one can construct the corresponding lines in the $\Lambda_1 - \Lambda_2$ diagram of the binary compact star merger GW170817 for which the individual masses M_1 and

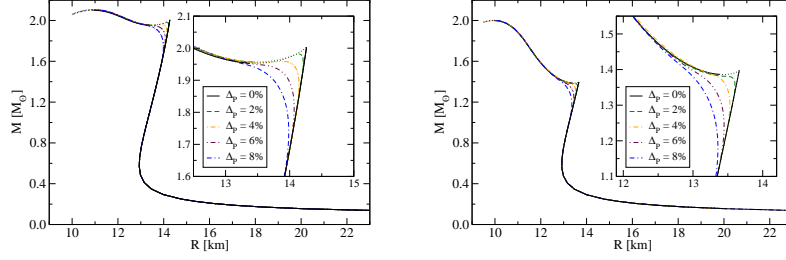


Fig. 1.6 Mass-radius diagram as a solution of the TOV equations for the equations of state ACB4 (left panel) which exhibits high mass twin stars and ACB5 (right panel) which describes low mass twins, depending on the value of the mixed phase parameter Δ_P .

M_2 of the two compact stars fulfill the constraint derived from the detected gravitational wave signal of the inspiral phase of the merger [Abbott *et al.* (2017)]. These lines can be overlaid to the constraint derived from the LVC observation, as shown in Fig. 1.7. As to be expected from Fig. 1.6, only in the case of ACB5 we can note an effect of the mixed phase construction while the results for ACB4 are inert against changes of the mixed phase parameter, because it influences the mass-radius diagram in a region of masses that is inaccessible to the gravitational wave signal of the inspiral phase and the effects of tidal deformation. Moreover, we notice that ACB4 is too stiff an EoS to fulfil the compactness constraint from GW170817. The EoS ACB5, however, with the early onset of the phase transition, becomes a soft EoS due to the mixed phase effects and for the largest values of the mixed phase parameter Δ_P is similar to a soft hadronic EoS despite the fact that the compact stars consist of extended regions of quark matter in pure or mixed phases.

In the following section, we will consider the effects of fast rotation on the sequences of hybrid star solutions and shall obtain a qualitative difference in the characteristics of pure phase (hadronic) and hybrid stars concerning their maximum masses which are relevant for the discussion of the phenomenology of binary compact star mergers and their implications for the state of superdense matter.

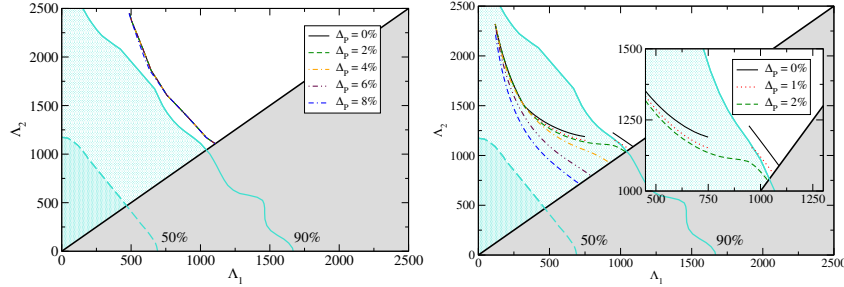


Fig. 1.7 Tidal deformability constraint from GW170817 for equations of state for high mass twins (left) and low mass twins (right).

1.5.3 Rotating compact star solutions

In this subsection we present the numerical solutions for rotating hybrid star sequences in full GR equations for axial symmetry as obtained with the RNS code described in subsection 1.2.2 and in the perturbative expansion up to order Ω^2 (slow rotation approximation) that was explained in subsection 1.2.3. We relate these solutions to those of the TOV equations for the static case of spherical symmetry discussed in the previous subsection 1.2.4.

In Fig. 1.8 we show the gravitational mass as a function of the central energy density for both multipolytrope EoS, ACB4 (with a deconfinement phase transition at high-mass, upper panels) and ACB5 (with a transition at the typical compact star mass of $1.4 M_\odot$, lower panels) for nonrotating (blue solid lines) and maximally rotating ($\Omega = \Omega_K$) stars in full GR (red dashed lines) and slow rotation approximation (orange dash-dotted line). In the left panels for the Maxwell construction case the jump in the central energy density by about a factor two at the onset of the transition is clearly seen and such an amount of latent heat is sufficient, according to the Seidov criterion Eq. (1.1), to trigger a gravitational instability which occurs in the region of densities where

$$\frac{dM}{d\varepsilon} < 0. \quad (1.70)$$

At the onset of this instability the gravitational mass of the star has reached the maximum attainable on the second family of compact stars, denoted by $M_{\text{max},2}$. For the Maxwell construction case, this mass is degenerate with that for the onset of the phase transition, M_{onset} . Due to the absence of a pressure gradient in the interval of densities corresponding to the mixed phase, this phase is not realized in compact stars in this case. The EoS with mass twin compact star sequences are characterized by the fact that the

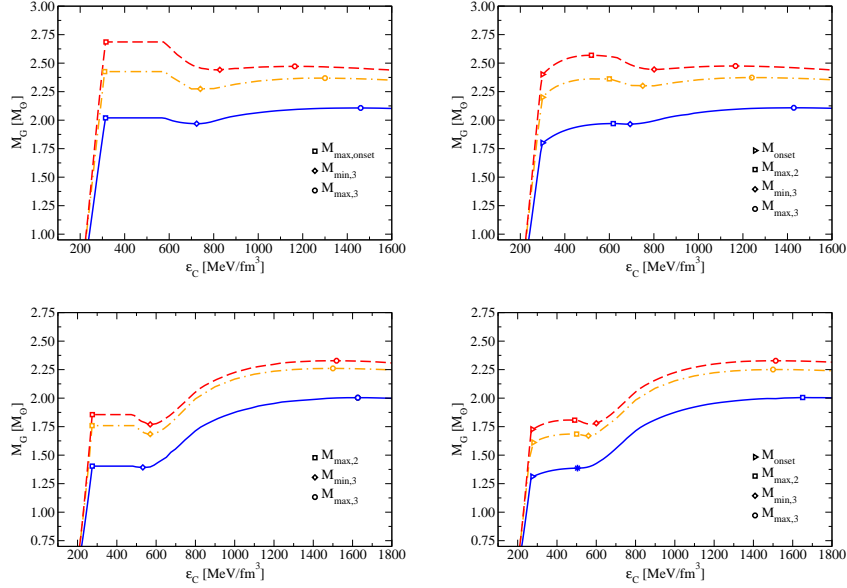


Fig. 1.8 The Mass–central energy density diagram for compact star configurations for the EoS ACB4 (upper panels) and ACB5 (lower panels). The *left* panels are for $\Delta_P = 0$ (Maxwell construction) and the *right* ones are for the critical value of the mixed-phase parameter ($\Delta_P = 0.04$ for ACB4 and $\Delta_P = 0.02$ for ACB5) for which the third family vanishes in the static case because it joins the second family of neutron stars. Each panel shows three curves: the solution of the TOV equations for the static case (blue solid line), the solution of the slow rotation case (Ω^2 approximation) for rotation at the Kepler frequency Ω_K (orange dash-dotted line) and the full solution of the axisymmetric Einstein equations with the RNS code for $\Omega = \Omega_K$ (red dashed line). The symbols denote the onset mass for deconfinement (triangle right), the maximum mass on the 2nd family branch (square), the minimum mass (diamond) and the maximum mass (circle) on the 3rd family branch.

instability criterion (1.70) is fulfilled in a finite interval of densities which is then followed by another stable, rising branch of sequences, the so-called third family of compact stars. This behavior defines two more characteristic masses: $M_{\min,3}$ at the lower and $M_{\max,3}$ at the upper turning point, see the left panels of Fig. 1.8.

For the mixed phase constructions depicted in the right panels of Fig. 1.8, the pressures at the onset and the end of the mixed phase are not identical and thus, due to the corresponding pressure gradient, a mixed phase can be realized in the star and the degeneracy between M_{onset} and

$M_{\max,2}$ is lifted. On the other hand, by our choice of the value of the mixed phase parameter Δ_P close to the limiting value for which the second and the third families of compact stars would get connected, the instability vanishes and thus $M_{\min,3}$ joins $M_{\max,2}$, so that for a slightly larger value of Δ_P both these masses can no longer be identified since only the second family survives which for $M > M_{\text{onset}}$ consists of hybrid stars.

These four characteristic masses for a given mass twin compact star EoS are given in Tab. 1.4 for the static case obtained by solving the TOV equations. In the last column the absolute maximum of the mass-radius curve for the given EoS is listed. In tables 1.5 and 1.6 these five characteristic masses are listed for the sequences of stars rotating at the Kepler frequency Ω_K which are obtained from solutions of the axisymmetric Einstein equations in the Ω^2 approximation and in full General Relativity, respectively.

Table 1.4 Five characteristic masses extracted from solutions of the Tolman-Oppenheimer-Volkoff equations (superscript "TOV") for sequences of static configurations with the EoS ACB4 and ACB5 for the Maxwell construction case ($\Delta_P = 0$) and for the mixed phase construction with the limiting value of Δ_P for which the second and the third family branches join. M_{onset} is the maximum mass of the purely hadronic second family branch at the onset of deconfinement, $M_{\max,2}$ denotes the maximum mass reached at the end of the mixed phase, $M_{\min,3}$ and $M_{\max,3}$ are the minimum and the maximum mass on the third family branch of the sequence. The maximum mass of the whole sequence for a given EoS is denoted as M_{\max} .

EoS	Δ_P	$M_{\max,\text{ons}}^{\text{TOV}}$	$M_{\max,2}^{\text{TOV}}$	$M_{\min,3}^{\text{TOV}}$	$M_{\max,3}^{\text{TOV}}$	M_{\max}^{TOV}
ACB4	0%	2.020	2.020	1.969	2.107	2.107
	4%	1.801	1.970	1.965	2.108	2.108
ACB5	0%	1.404	1.404	1.393	2.004	2.004
	2%	1.312	1.386*	1.386*	2.006*	2.006

Table 1.5 Same as Table 1.4, but now for solutions of the axisymmetric Einstein equations in the slow rotation approximation, the perturbative expansion to order Ω^2 denoted by the corresponding superscript.

EoS	Δ_P	$M_{\max,\text{ons}}^{\Omega^2}$	$M_{\max,2}^{\Omega^2}$	$M_{\min,3}^{\Omega^2}$	$M_{\max,3}^{\Omega^2}$	$M_{\max}^{\Omega^2}$
ACB4	0%	2.426	2.426	2.274	2.369	2.426
	4%	2.200	2.362	2.301	2.373	2.373
ACB5	0%	1.759	1.759	1.685	2.261	2.261
	2%	1.611	1.685	1.670	2.251	2.251

Table 1.6 Same as Table 1.4, but now for solutions of the full system of Einstein equations for uniform rotation in axial symmetry [Cook *et al.* (1994)] using the RNS code. The corresponding results are denoted by the superscript "rot".

EoS	Δ_P	$M_{\text{onset}}^{\text{rot}}$	$M_{\text{max},2}^{\text{rot}}$	$M_{\text{min},3}^{\text{rot}}$	$M_{\text{max},3}^{\text{rot}}$	$M_{\text{max}}^{\text{rot}}$
ACB4	0%	2.686	2.686	2.442	2.472	2.686
	4%	2.401	2.569	2.445	2.475	2.569
ACB5	0%	1.855	1.855	1.770	2.328	2.328
	2%	1.727	1.807	1.780	2.328	2.328

Inspecting the rotating star sequences for the close-to-critical mixed phase parameter Δ_P , we observe that due to the rotation the star branches with mixed phase and pure quark matter core can get disconnected so that the phenomenon of a third family reappears. Vice-versa, upon spin-down from a supramassive star configuration at maximal rotation frequency (created, e.g., in a binary neutron star merger) which is stable on the hadronic or mixed phase branch may end up either as a black hole or on the hybrid star branch for such mixed-phase EoS. The scenario of a delayed collapse to a black hole is of special importance for interpreting GW170817 and will therefore be discussed below in further detail. In this context appears the question whether between the above-introduced characteristic masses at maximal and at zero rotation frequency hold EoS-independent, so-called *universal relations* that have been investigated for the maximum mass of hadronic EoS [Bozzola *et al.* (2018); Rezzolla *et al.* (2018)] and recently also for hybrid EoS including the Maxwell construction cases of ACB4 and ACB5 [Bozzola *et al.* (2019)]. We shall come back to this issue below.

Here we like to remark that the maximum masses on the second and third family branches correspond to stars with very different central (energy) densities. This may be the clue to understanding the fact that the increase in mass for stars on the more compact third family branch is smaller than for stars on the second family one because of their smaller radii and thus smaller moment of inertia (1.53) and rotational energy, see the gravitational mass vs. equatorial radius in Fig. 1.9. For a more quantitative discussion of the effects of rotation on the masses of the sequences, we extract from the tables 1.4-1.6 the ratios of the characteristic masses on the rotating sequences to those on the static ones in table 1.7 and table 1.8 for the Ω^2 approximation and the full GR solution, respectively. For completeness, we give the ratio of the characteristic masses between the two rotation solutions in table 1.9.

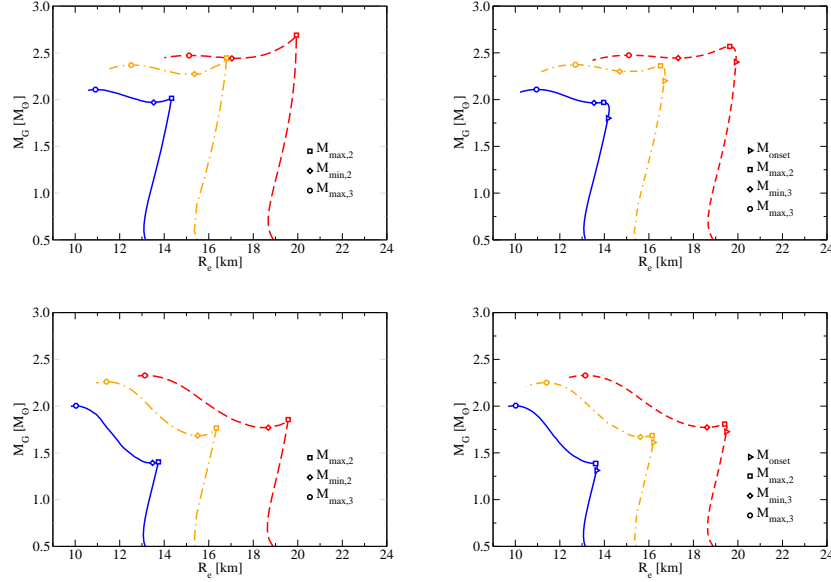


Fig. 1.9 The Mass–Radius diagram for compact star configurations for the EoS ACB4 (upper panels) and ACB5 (lower panels). The *left* panels are for $\Delta_P = 0$ (Maxwell construction) and the *right* ones are for the critical value of the mixed-phase parameter ($\Delta_P = 0.04$ for ACB4 and $\Delta_P = 0.02$ for ACB5) for which the third family vanishes in the static case because it joins the second family of neutron stars. Each panel shows three curves: the solution of the TOV equations for the static case (blue solid line), the solution of the slow rotation case (Ω^2 approximation) for rotation at the Kepler frequency Ω_K (orange dash-dotted line) and the full solution of the axisymmetric Einstein equations with the RNS code for $\Omega = \Omega_K$ (red dashed line). The symbols denote the onset mass for deconfinement (triangle right), the maximum mass on the 2nd family branch (square), the minimum mass (diamond) and the maximum mass (circle) on the 3rd family branch.

1.6 Implications for the phenomenology of compact stars

We investigate the consequences of a strong phase transition in the EoS for dense compact star matter for sequences of configurations in the mass-radius as well as mass-central (energy) density plane, with and without rotation. While for isolated pulsars even the highest known spin frequencies are well below the Kepler frequency so that no strong modification of the TOV solution occurs, in the era of multi-messenger astronomy, with compact star mergers being accessible to detection by their GW signal from the inspiral phase and soon also from the postmerger state, the ”übermassive”

[Espino and Paschalidis (2019)] as well as supramassive star solutions play a role in the interpretation of the observations. While the former are solutions for differentially rotating configurations at the mass shedding limit, the latter are uniformly rotating objects with a frequency close to the Kepler one [Shibata *et al.* (2019)]. Recently, for this case EoS independent, so-called "universal" relationships have been derived which relate the max-

Table 1.7 Ratios formed by the five characteristic masses at maximal rotation frequency Ω_K in the slow rotation approximation (superscript " Ω^2 ") relative to the static case (superscript "TOV") calculated with the EoS ACB4 and ACB5 for the Maxwell construction case ($\Delta_P = 0$) and for the mixed phase construction with the limiting value of Δ_P .

EoS	Δ_P	$\frac{M_{\text{ons}}^{\Omega^2}}{M_{\text{ons}}^{\text{TOV}}}$	$\frac{M_{\text{max},2}^{\Omega^2}}{M_{\text{max},2}^{\text{TOV}}}$	$\frac{M_{\text{min},3}^{\Omega^2}}{M_{\text{min},3}^{\text{TOV}}}$	$\frac{M_{\text{max},3}^{\Omega^2}}{M_{\text{max},3}^{\text{TOV}}}$	$\frac{M_{\text{max}}^{\Omega^2}}{M_{\text{max}}^{\text{TOV}}}$
ACB4	0%	1.201	1.201	1.155	1.124	1.151
	4%	1.222	1.199	1.171	1.126	1.126
ACB5	0%	1.253	1.253	1.210	1.128	1.128
	2%	1.228	1.216*	1.205*	1.122*	1.122

Table 1.8 Same as Table 1.7, but now for the full solutions of the axisymmetric Einstein equations with the RNS code relative to the solutions of the TOV equations for the static case.

EoS	Δ_P	$\frac{M_{\text{ons}}^{\text{rot}}}{M_{\text{ons}}^{\text{TOV}}}$	$\frac{M_{\text{max},2}^{\text{rot}}}{M_{\text{max},2}^{\text{TOV}}}$	$\frac{M_{\text{min},3}^{\text{rot}}}{M_{\text{min},3}^{\text{TOV}}}$	$\frac{M_{\text{max},3}^{\text{rot}}}{M_{\text{max},3}^{\text{TOV}}}$	$\frac{M_{\text{max}}^{\text{rot}}}{M_{\text{max}}^{\text{TOV}}}$
ACB4	0%	1.330	1.330	1.240	1.173	1.275
	4%	1.333	1.304	1.244	1.174	1.174
ACB5	0%	1.321	1.321	1.270	1.162	1.162
	2%	1.316	1.304*	1.284*	1.161*	1.161

Table 1.9 Same as Table 1.7, but now the full solutions of the axisymmetric Einstein equations (superscript "RNS") are related to those in the slow rotation approximation (superscript Ω^2).

EoS	Δ_P	$\frac{M_{\text{ons}}^{\text{rot}}}{M_{\text{ons}}^{\Omega^2}}$	$\frac{M_{\text{max},2}^{\text{rot}}}{M_{\text{max},2}^{\Omega^2}}$	$\frac{M_{\text{min},3}^{\text{rot}}}{M_{\text{min},3}^{\Omega^2}}$	$\frac{M_{\text{max},3}^{\text{rot}}}{M_{\text{max},3}^{\Omega^2}}$	$\frac{M_{\text{max}}^{\text{rot}}}{M_{\text{max}}^{\Omega^2}}$
ACB4	0%	1.107	1.107	1.074	1.043	1.107
	4%	1.091	1.087	1.063	1.043	1.082
ACB5	0%	1.054	1.054	1.050	1.030	1.030
	2%	1.072	1.072	1.065	1.034	1.034

imum mass of the supramassive star sequence to the static one from the solution of the TOV equation. Such relationships, once confirmed, are particularly useful in order to make general predictions or draw conclusions from merger phenomenology for constraints limiting the EoS properties. In this context we would like to mention the upper limit on the maximum mass of neutron stars that has been extracted from the GW signal and phenomenology of GW170817 [Shibata *et al.* (2017); Margalit and Metzger (2017); Rezzolla *et al.* (2018)].

It has been known since long [Haensel *et al.* (2007)] that there is a relationship between the maximum mass of uniformly rotating cold neutron stars at the maximum frequency and the maximum mass of the TOV equation solution for static stars as

$$M_{\max}(\Omega_K) = \alpha M_{\max}^{\text{TOV}}, \quad (1.71)$$

where recently in Ref. [Breu and Rezzolla (2016)] the universality of this relationship was confirmed for a very large set of hadronic EoS (without a deconfinement phase transition) with the coefficient $\alpha = 1.20$. The hypothesis that the relation (1.71) can be extended to include hybrid stars with a strong phase transition and even with third family sequences has recently been investigated in Ref. [Bozzola *et al.* (2019)] and following the argumentation of [Ruiz *et al.* (2018); Most *et al.* (2018); Rezzolla *et al.* (2018)] it leads to a limitation for the maximum mass of static neutron stars as

$$2.07 M_{\odot} \simeq M_{\max}^{\text{TOV}} \simeq 2.23 M_{\odot}. \quad (1.72)$$

The value of $M_{\max} = 2.591 M_{\odot}$ was extracted for the core mass of the compact star merger GW170817 in Ref. [Rezzolla *et al.* (2018)]. We confirm the finding of [Bozzola *et al.* (2019)] that the coefficient spans a range of values for which we find $1.16 < \alpha < 1.33$, see the table 1.8. The lower limit in (1.72) comes from the new high-mass pulsar PSR J0740+6620 for which a mass $2.17_{-0.10}^{+0.11} M_{\odot}$ has been determined by Cromartie *et al.* (2019) by measuring the Shapiro delay, and the upper limit in our case is $2.23 M_{\odot}$ for the lowest value of $\alpha = 1.16$. In order to not come in conflict with the pulsar mass measurement of (Cromartie *et al.*, 2019), there is an upper limit for the admissible value of $\alpha = 1.25$, corresponding to the lower limit at the 1σ level of the PSR J0740+6620 mass, $M_{\max}^{\text{TOV}} = 2.07 M_{\odot}$. Taking the central value, $M_{\max}^{\text{TOV}} = 2.17 M_{\odot}$, would correspond to $\alpha = 1.20$, see Fig. 1.10. This figure illustrates one of the main findings of this contribution, the dependence of the coefficient α in Eq. (1.71) on the central (energy) density of the stellar configuration that can be fitted by a linear regression to the

values we determined at the positions corresponding to the characteristic masses to be

$$\alpha = a - b\varepsilon_c, \quad (1.73)$$

where $a_{ACB4-4} = 1.38 \pm 0.07$, $b_{ACB4-4} = 0.12 \pm 0.01 \text{ fm}^3/\text{GeV}$ and $a_{ACB5-2} = 1.37 \pm 0.07$, $b_{ACB5-2} = 0.16 \pm 0.02 \text{ fm}^3/\text{GeV}$.

We may conclude that only those states of matter are allowed for the inner core of a compact star at maximum mass of $2.07 M_\odot$ ($2.17 M_\odot$) which belong to a high-density region with $\varepsilon \geq 0.78 \text{ GeV}/\text{fm}^3$ ($\varepsilon \geq 1.12 \text{ GeV}/\text{fm}^3$).

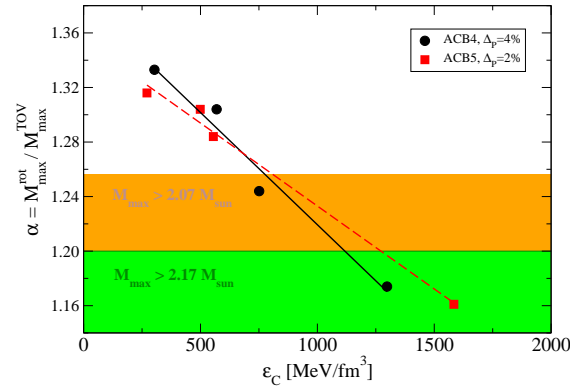


Fig. 1.10 Ratio of the mass for maximally rotating stars to that of a static star as a function of the central energy density. For a comparison the value 1.20 would be the maximum value compatible with a lower limit on the maximum mass of (nonrotating) pulsars of $2.17 M_\odot$ [Cromartie *et al.* (2019)].

Anyway, the main effect of the strong phase transition is a higher compactness of the high mass stars than in the purely hadronic case which moreover goes along with a smaller mass increase due to maximal rotation than in the purely hadronic case which entails the increase of the upper limit for the maximum mass relative to the purely hadronic case discussed in [Shibata *et al.* (2017); Margalit and Metzger (2017); Rezzolla *et al.* (2018)]. Thus the high-density phase transition removes a certain tension from the discussion of the upper limit for the maximum mass and could be used as an argument in favour of the suggestion that a strong phase transition actually takes place in compact stars!

1.7 Summary and Conclusions

Stimulated by the unprecedented progress in observational astronomy, compact stars have become superb astrophysical laboratories for a broad range of physical studies. This is particularly the case for neutron stars, since their observables carry information about the fundamental building blocks of matter and even of the fabric of space itself. Against this background we did present in this book chapter a systematic investigation of the properties of compact stellar mass twins (i.e., the so-called third family of compact stars), which, according to theory, may exist in the mass-radius region between neutron stars and stellar-mass black holes. Particular emphasis is given to modeling the rotational properties of compact mass twins for multi-polytrope models for the equation of state of ultra-dense stellar matter that fulfill the constraint established for the maximum mass of a neutron star. The main results of our investigation can be summarized as follows:

- 1) The existence of mass twins invariably signals the existence of a strong phase transition in ultra-dense matter. The extreme softening of the equation of state caused by the strong phase transition increases the gravitational field so much that the star becomes gravitationally unstable over a certain range of densities, where just a certain fraction of the star's core is in the new high-density phase. Eventually the stars becomes stable again when about half of the matter in its core is in the new phase of matter. The new stars have gravitational masses that are less than the maximal mass of the hadronic stellar sequence.

The observation of mass twins would indicate a strong phase transition so that from the existence of a strong first-order phase transition in one corner of the QCD phase diagram and a crossover behavior in another, one could conclude that at least one critical endpoint (CEP) must exist. This would be very reassuring for large scale experimental heavy-ion collision programs set up for the search for the CEP.

- 2) The mixed phase construction which mimics the pasta phase is in accordance with a full pasta calculation. The result is a "smearing" of the phase transition over a certain pressure region, which is similar to the Gibbs construction in matter with more than one conserved charge and where charge conservation need not be fulfilled locally but rather globally [Glendenning (1992)]. This construction makes not only the approach to the strong phase transition more realistic, but has also great advantages for the numerical realization of phenomenological scenarios of the phase transition in rapidly rotating stars studied in numerical relativity.

3) Lastly, we address the conjecture of an upper limit on the maximum masses of nonrotating compact stars from the phenomenology of GW170817 and its associated kilonova event. The conjecture is based on a quasi-universal relation between the maximum masses of uniformly rotating stars at the maximum frequency and that of static TOV solutions for the same EoS, which was demonstrated to hold for neutron star EoS without a phase transition [Breu and Rezzolla (2016)]. The stellar mass at which the high-density phase transition (such as deconfinement of quarks) sets in is currently unknown. But if the transition would occur below the maximum mass of the TOV solution, the quasi-universal relation will have to be revisited and the conclusions for the upper limit on the maximum mass be revised. We have found a quantitative criterion for the minimal central energy density in the maximum-mass configuration of a compact star that would correspond to the core of GW170817 after dynamical mass ejection [Rezzolla *et al.* (2018)]. Thus the EoS at high densities must be effectively soft, either in the form of a relatively soft hadronic EoS or as a hybrid EoS with a phase transition, since a too stiff a hadronic EoS would lead to heavy hadronic stars too dilute to fulfill the constraint derived by us.

With these prospects for strong gravity and strong phase transitions in compact stars, we are looking forward to the next series of exciting discoveries in the just opened era of multimessenger astronomy.

Acknowledgements

We would like to thank Andreas Bauswein for helpful discussions and Vasilis Paschalidis for pointing out caveats in the discussion of the maximum mass constraint from GW170817. We are grateful to Cesar Zen Vasconcellos for the invitation to contribute to this book and for his steady encouragement to complete the writeup despite interfering obligations. The work of D.B., A.A., H.G. has been supported by the Russian Science Foundation under grant 17-12-01427; F.W. acknowledges support by the U.S. National Science Foundation under Grant PHY-1714068. The authors are grateful to the European COST Actions CA15213 "THOR" and CA16214 "PHAROS" for supporting their networking activities.

Bibliography

- Abbott, B. *et al.* (2017). GW170817: Observation of Gravitational Waves from a Binary Neutron Star Inspiral, *Phys. Rev. Lett.* **119**, 16, p. 161101, doi:10.1103/PhysRevLett.119.161101, [arXiv:1710.05832 \[gr-qc\]](#).
- Abgaryan, V., Alvarez-Castillo, D., Ayriyan, A., Blaschke, D., and Grigorian, H. (2018). Two Novel Approaches to the Hadron-Quark Mixed Phase in Compact Stars, *Universe* **4**, 9, p. 94, doi:10.3390/universe4090094, [arXiv:1807.08034 \[astro-ph.HE\]](#).
- Alford, M. G., Burgio, G. F., Han, S., Taranto, G., and Zappala, D. (2015). Constraining and applying a generic high-density equation of state, *Phys. Rev.* **D92**, 8, p. 083002, doi:10.1103/PhysRevD.92.083002, [arXiv:1501.07902 \[nucl-th\]](#).
- Alford, M. G. and Han, S. (2016). Characteristics of hybrid compact stars with a sharp hadron-quark interface, *Eur. Phys. J.* **A52**, 3, p. 62, doi:10.1140/epja/i2016-16062-9, [arXiv:1508.01261 \[nucl-th\]](#).
- Alford, M. G., Han, S., and Prakash, M. (2013). Generic conditions for stable hybrid stars, *Phys. Rev.* **D88**, 8, p. 083013, doi:10.1103/PhysRevD.88.083013, [arXiv:1302.4732 \[astro-ph.SR\]](#).
- Alford, M. G. and Sedrakian, A. (2017). Compact stars with sequential QCD phase transitions, *Phys. Rev. Lett.* **119**, 16, p. 161104, doi:10.1103/PhysRevLett.119.161104, [arXiv:1706.01592 \[astro-ph.HE\]](#).
- Alvarez-Castillo, D. E., Bejger, M., Blaschke, D., Haensel, P., and Zdunik, L. (2015). Energy bursts from deconfinement in high-mass twin stars, [arXiv:1506.08645 \[astro-ph.HE\]](#).
- Alvarez-Castillo, D. E. and Blaschke, D. (2013). Proving the CEP with compact stars? in *Proceedings, 17th Conference of Young Scientists and Specialists (AYSS '13): Dubna, Russia, April 8-12, 2013*, [arXiv:1304.7758 \[astro-ph.HE\]](#).
- Alvarez-Castillo, D. E. and Blaschke, D. B. (2017). High-mass twin stars with a multipolytrope equation of state, *Phys. Rev.* **C96**, 4, p. 045809, doi:10.1103/PhysRevC.96.045809, [arXiv:1703.02681 \[nucl-th\]](#).
- Alvarez-Castillo, D. E., Blaschke, D. B., Grunfeld, A. G., and Pagura, V. P. (2019). Third family of compact stars within a nonlocal chiral quark model

- equation of state, *Phys. Rev.* **D99**, 6, p. 063010, doi:10.1103/PhysRevD.99.063010, arXiv:1805.04105 [hep-ph].
- Annala, E., Gorda, T., Kurkela, A., and Vuorinen, A. (2018). Gravitational-wave constraints on the neutron-star-matter Equation of State, *Phys. Rev. Lett.* **120**, 17, p. 172703, doi:10.1103/PhysRevLett.120.172703, arXiv:1711.02644 [astro-ph.HE].
- Arzoumanian, Z. *et al.* (2009). X-ray Timing of Neutron Stars, Astrophysical Probes of Extreme Physics, arXiv:0902.3264 [astro-ph.HE].
- Ayriyan, A., Bastian, N. U., Blaschke, D., Grigorian, H., Maslov, K., and Voskresensky, D. N. (2018). Robustness of third family solutions for hybrid stars against mixed phase effects, *Phys. Rev.* **C97**, 4, p. 045802, doi:10.1103/PhysRevC.97.045802, arXiv:1711.03926 [nucl-th].
- Ayriyan, A. and Grigorian, H. (2018). Model of the Phase Transition Mimicking the Pasta Phase in Cold and Dense Quark-Hadron Matter, *EPJ Web Conf.* **173**, p. 03003, doi:10.1051/epjconf/201817303003, arXiv:1710.05637 [astro-ph.HE].
- Ayvazyan, N. S., Colucci, G., Rischke, D. H., and Sedrakian, A. (2013). Rotating hybrid compact stars, *Astron. Astrophys.* **559**, p. A118, doi:10.1051/0004-6361/201322484, arXiv:1308.3053 [astro-ph.SR].
- Bauswein, A., Just, O., Janka, H.-T., and Stergioulas, N. (2017). Neutron-star radius constraints from GW170817 and future detections, *Astrophys. J.* **850**, 2, p. L34, doi:10.3847/2041-8213/aa9994, arXiv:1710.06843 [astro-ph.HE].
- Baym, G., Hatsuda, T., Kojo, T., Powell, P. D., Song, Y., and Takatsuka, T. (2018). From hadrons to quarks in neutron stars: a review, *Rept. Prog. Phys.* **81**, 5, p. 056902, doi:10.1088/1361-6633/aaae14, arXiv:1707.04966 [astro-ph.HE].
- Bejger, M., Blaschke, D., Haensel, P., Zdunik, J. L., and Fortin, M. (2017). Consequences of a strong phase transition in the dense matter equation of state for the rotational evolution of neutron stars, *Astron. Astrophys.* **600**, p. A39, doi:10.1051/0004-6361/201629580, arXiv:1608.07049 [astro-ph.HE].
- Benic, S. (2014). Heavy hybrid stars from multi-quark interactions, *Eur. Phys. J.* **A50**, p. 111, doi:10.1140/epja/i2014-14111-1, arXiv:1401.5380 [nucl-th].
- Benic, S., Blaschke, D., Alvarez-Castillo, D. E., Fischer, T., and Typel, S. (2015). A new quark-hadron hybrid equation of state for astrophysics - I. High-mass twin compact stars, *Astron. Astrophys.* **577**, p. A40, doi:10.1051/0004-6361/201425318, arXiv:1411.2856 [astro-ph.HE].
- Benic, S., Blaschke, D., Contrera, G. A., and Horvatic, D. (2014). Medium induced Lorentz symmetry breaking effects in nonlocal Polyakov?Nambu?Jona-Lasinio models, *Phys. Rev.* **D89**, 1, p. 016007, doi:10.1103/PhysRevD.89.016007, arXiv:1306.0588 [hep-ph].
- Binnington, T. and Poisson, E. (2009). Relativistic theory of tidal Love numbers, *Phys. Rev.* **D80**, p. 084018, doi:10.1103/PhysRevD.80.084018, arXiv:0906.1366 [gr-qc].
- Blaschke, D., Alvarez-Castillo, D. E., and Benic, S. (2013a). Mass-radius con-

- straints for compact stars and a critical endpoint, *PoS CPOD2013*, p. 063, doi:10.22323/1.185.0063, arXiv:1310.3803 [nucl-th].
- Blaschke, D., Alvarez Castillo, D. E., Benic, S., Contrera, G., and Lastowiecki, R. (2013b). Nonlocal PNJL models and heavy hybrid stars, doi:10.22323/1.171.0249, arXiv:1302.6275 [hep-ph], [PoSConfinementX,249(2012)].
- Blaschke, D. B., Gomez Dumm, D., Grunfeld, A. G., Klahn, T., and Scoccola, N. N. (2007). Hybrid stars within a covariant, nonlocal chiral quark model, *Phys. Rev.* **C75**, p. 065804, doi:10.1103/PhysRevC.75.065804, arXiv:nucl-th/0703088 [nucl-th].
- Bozzola, G., Espino, P. L., Lewin, C. D., and Paschalidis, V. (2019). Maximum mass and universal relations of rotating relativistic hybrid hadron-quark stars, arXiv:1905.00028 [astro-ph.HE].
- Bozzola, G., Stergioulas, N., and Bauswein, A. (2018). Universal relations for differentially rotating relativistic stars at the threshold to collapse, *Mon. Not. Roy. Astron. Soc.* **474**, 3, pp. 3557–3564, doi:10.1093/mnras/stx3002, arXiv:1709.02787 [gr-qc].
- Breu, C. and Rezzolla, L. (2016). Maximum mass, moment of inertia and compactness of relativistic stars, *Mon. Not. Roy. Astron. Soc.* **459**, 1, pp. 646–656, doi:10.1093/mnras/stw575, arXiv:1601.06083 [gr-qc].
- Christian, J.-E., Zacchi, A., and Schaffner-Bielich, J. (2018). Classifications of Twin Star Solutions for a Constant Speed of Sound Parameterized Equation of State, *Eur. Phys. J.* **A54**, 2, p. 28, doi:10.1140/epja/i2018-12472-y, arXiv:1707.07524 [astro-ph.HE].
- Christian, J.-E., Zacchi, A., and Schaffner-Bielich, J. (2019). Signals in the tidal deformability for phase transitions in compact stars with constraints from GW170817, *Phys. Rev.* **D99**, 2, p. 023009, doi:10.1103/PhysRevD.99.023009, arXiv:1809.03333 [astro-ph.HE].
- Chubarian, E., Grigorian, H., Poghosyan, G. S., and Blaschke, D. (2000). Deconfinement phase transition in rotating nonspherical compact stars, *Astron. Astrophys.* **357**, pp. 968–976, arXiv:astro-ph/9903489 [astro-ph].
- Cook, G. B., Shapiro, S. L., and Teukolsky, S. A. (1994). Rapidly rotating polytropes in general relativity, *Astrophys. J.* **422**, pp. 227–242.
- Cromartie, H. T. *et al.* (2019). A very massive neutron star: relativistic Shapiro delay measurements of PSR J0740+6620, arXiv:1904.06759 [astro-ph.HE].
- Damour, T. and Nagar, A. (2009). Relativistic tidal properties of neutron stars, *Phys. Rev.* **D80**, p. 084035, doi:10.1103/PhysRevD.80.084035, arXiv:0906.0096 [gr-qc].
- Espino, P. and Paschalidis, V. (2019). Revisiting the maximum mass of differentially rotating neutron stars in general relativity with realistic equations of state, *Phys. Rev.* **D99**, 8, p. 083017, doi:10.1103/PhysRevD.99.083017, arXiv:1901.05479 [astro-ph.HE].
- Gerlach, U. H. (1968). Equation of State at Supranuclear Densities and the Existence of a Third Family of Superdense Stars, *Phys. Rev.* **172**, pp. 1325–1330, doi:10.1103/PhysRev.172.1325.
- Glendenning, N. K. (1992). First order phase transitions with more than one

- conserved charge: Consequences for neutron stars, *Phys. Rev.* **D46**, pp. 1274–1287, doi:10.1103/PhysRevD.46.1274.
- Glendenning, N. K. and Kettner, C. (2000). Nonidentical neutron star twins, *Astron. Astrophys.* **353**, p. L9, arXiv:astro-ph/9807155 [astro-ph].
- Glendenning, N. K. (2000). *Compact stars: Nuclear physics, particle physics, and general relativity* (Springer).
- Haensel, P., Potekhin, A. Y., and Yakovlev, D. G. (2007). Neutron stars I: Equation of state and structure, *Astrophys. Space Sci. Libr.* **326**, pp. pp.1–619, doi:10.1007/978-0-387-47301-7.
- Han, S. and Steiner, A. W. (2019). Tidal deformability with sharp phase transitions in (binary) neutron stars, *Phys. Rev.* **D99**, 8, p. 083014, doi:10.1103/PhysRevD.99.083014, arXiv:1810.10967 [nucl-th].
- Hanauske, M., Yilmaz, Z. S., Mitropoulos, C., Rezzolla, L., and Stöcker, H. (2018). Gravitational waves from binary compact star mergers in the context of strange matter, in *European Physical Journal Web of Conferences, European Physical Journal Web of Conferences*, Vol. 171, p. 20004, doi:10.1051/epjconf/201817120004.
- Hartle, J. B. (1967). Slowly rotating relativistic stars. I. Equations of structure, *Astrophys. J.* **150**, pp. 1005–1029, doi:10.1086/149400.
- Hartle, J. B. and Thorne, K. S. (1968). Slowly Rotating Relativistic Stars. II. Models for Neutron Stars and Supermassive Stars, *Astrophys. J.* **153**, p. 807, doi:10.1086/149707.
- Haskell, B. and Melatos, A. (2015). Models of Pulsar Glitches, *Int. J. Mod. Phys.* **D24**, 03, p. 1530008, doi:10.1142/S0218271815300086, arXiv:1502.07062 [astro-ph.SR].
- Hebeler, K., Lattimer, J. M., Pethick, C. J., and Schwenk, A. (2010). Constraints on neutron star radii based on chiral effective field theory interactions, *Phys. Rev. Lett.* **105**, p. 161102, doi:10.1103/PhysRevLett.105.161102, arXiv:1007.1746 [nucl-th].
- Hebeler, K., Lattimer, J. M., Pethick, C. J., and Schwenk, A. (2013). Equation of state and neutron star properties constrained by nuclear physics and observation, *Astrophys. J.* **773**, p. 11, doi:10.1088/0004-637X/773/1/11, arXiv:1303.4662 [astro-ph.SR].
- Hinderer, T. (2008). Tidal Love numbers of neutron stars, *Astrophys. J.* **677**, pp. 1216–1220, doi:10.1086/533487, arXiv:0711.2420 [astro-ph].
- Hinderer, T., Lackey, B. D., Lang, R. N., and Read, J. S. (2010). Tidal deformability of neutron stars with realistic equations of state and their gravitational wave signatures in binary inspiral, *Phys. Rev.* **D81**, p. 123016, doi:10.1103/PhysRevD.81.123016, arXiv:0911.3535 [astro-ph.HE].
- Horowitz, C. J., Moniz, E. J., and Negele, J. W. (1985). HADRON STRUCTURE IN A SIMPLE MODEL OF QUARK / NUCLEAR MATTER, *Phys. Rev.* **D31**, pp. 1689–1699, doi:10.1103/PhysRevD.31.1689.
- Kaltenborn, M. A. R., Bastian, N.-U. F., and Blaschke, D. B. (2017). Quark-nuclear hybrid star equation of state with excluded volume effects, *Phys. Rev.* **D96**, 5, p. 056024, doi:10.1103/PhysRevD.96.056024, arXiv:1701.04400 [astro-ph.HE].

- Komatsu, H., Eriguchi, Y., and Hachisu, I. (1989). Rapidly rotating general relativistic stars. I - Numerical method and its application to uniformly rotating polytropes, *Mon. Not. Roy. Astron. Soc.* **237**, pp. 355–379.
- Laarakkers, W. G. and Poisson, E. (1999). Quadrupole moments of rotating neutron stars, *Astrophys. J.* **512**, pp. 282–287, doi:10.1086/306732, arXiv:gr-qc/9709033 [gr-qc].
- Lattimer, J. M. and Prakash, M. (2007). Neutron Star Observations: Prognosis for Equation of State Constraints, *Phys. Rept.* **442**, pp. 109–165, doi:10.1016/j.physrep.2007.02.003, arXiv:astro-ph/0612440 [astro-ph].
- Lindblom, L. (1998). Phase transitions and the mass radius curves of relativistic stars, *Phys. Rev.* **D58**, p. 024008, doi:10.1103/PhysRevD.58.024008, arXiv:gr-qc/9802072 [gr-qc].
- M. Spinella, W., Weber, F., A. Contrera, G., and G. Orsaria, M. (2016). Neutrino emissivity in the quark-hadron mixed phase of neutron stars, *Eur. Phys. J. A* **52**, 3, doi:10.1140/epja/i2016-16061-x, <https://www.scopus.com/inward/record.uri?eid=2-s2.0-84962492783&doi=10.1140>, cited By 3.
- Margalit, B. and Metzger, B. D. (2017). Constraining the Maximum Mass of Neutron Stars From Multi-Messenger Observations of GW170817, *Astrophys. J.* **850**, 2, p. L19, doi:10.3847/2041-8213/aa991c, arXiv:1710.05938 [astro-ph.HE].
- Maslov, K., Yasutake, N., Ayriyan, A., Blaschke, D., Grigorian, H., Maruyama, T., Tatsumi, T., and Voskresensky, D. N. (2018). Hybrid equation of state with pasta phases and third family of compact stars I: Pasta phases and effective mixed phase model, arXiv:1812.11889 [nucl-th].
- Miller, M. C., Chirenti, C., and Lamb, F. K. (2019). Constraining the equation of state of high-density cold matter using nuclear and astronomical measurements, arXiv:1904.08907 [astro-ph.HE].
- Misner, C. W., Thorne, K. S., and Wheeler, J. A. (1973). *Gravitation* (W. H. Freeman, San Francisco), ISBN 9780716703440, 9780691177793.
- Montana, G., Tolos, L., Hanauske, M., and Rezzolla, L. (2019). Constraining twin stars with GW170817, *Phys. Rev.* **D99**, p. 103009, doi:10.1103/PhysRevD.99.103009, arXiv:1811.10929 [astro-ph.HE].
- Most, E. R., Weih, L. R., Rezzolla, L., and Schaffner-Bielich, J. (2018). New constraints on radii and tidal deformabilities of neutron stars from GW170817, *Phys. Rev. Lett.* **120**, 26, p. 261103, doi:10.1103/PhysRevLett.120.261103, arXiv:1803.00549 [gr-qc].
- Na, X., Xu, R., Weber, F., and Negreiros, R. (2012). Transport properties of a quark-hadron coulomb lattice in the cores of neutron stars, *Phys. Rev. D* **86**, 12, doi:10.1103/PhysRevD.86.123016, <https://www.scopus.com/inward/record.uri?eid=2-s2.0-84871596554&doi=10.1103>, cited By 10.
- Oppenheimer, J. R. and Volkoff, G. M. (1939). On Massive neutron cores, *Phys. Rev.* **55**, pp. 374–381, doi:10.1103/PhysRev.55.374.
- Orsaria, M., Rodrigues, H., Weber, F., and Contrera, G. A. (2014). Quark deconfinement in high-mass neutron stars, *Phys. Rev.* **C89**, 1, p. 015806, doi:10.1103/PhysRevC.89.015806, arXiv:1308.1657 [nucl-th].
- Paschalidis, V., Yagi, K., Alvarez-Castillo, D., Blaschke, D. B., and Sedrakian, A.

- (2018). Implications from GW170817 and I-Love-Q relations for relativistic hybrid stars, *Phys. Rev.* **D97**, 8, p. 084038, doi:10.1103/PhysRevD.97.084038, arXiv:1712.00451 [astro-ph.HE].
- Poghosyan, G. S., Grigorian, H., and Blaschke, D. (2001). Population clustering as a signal for deconfinement in accreting compact stars, *Astrophys. J.* **551**, p. L73, doi:10.1086/319851, arXiv:astro-ph/0101002 [astro-ph].
- Raithel, C. A., Ozel, F., and Psaltis, D. (2016). From Neutron Star Observables to the Equation of State: An Optimal Parametrization, *Astrophys. J.* **831**, 1, p. 44, doi:10.3847/0004-637X/831/1/44, arXiv:1605.03591 [astro-ph.HE].
- Ravenhall, D. G. and Pethick, C. J. (1994). Neutron Star Moments of Inertia, *Astrophysical Journal* **424**, p. 846, doi:10.1086/173935.
- Read, J. S., Lackey, B. D., Owen, B. J., and Friedman, J. L. (2009). Constraints on a phenomenologically parameterised neutron-star equation of state, *Phys. Rev.* **D79**, p. 124032, doi:10.1103/PhysRevD.79.124032, arXiv:0812.2163 [astro-ph].
- Rezzolla, L., Most, E. R., and Weih, L. R. (2018). Using gravitational-wave observations and quasi-universal relations to constrain the maximum mass of neutron stars, *Astrophys. J.* **852**, 2, p. L25, doi:10.3847/2041-8213/aaa401, arXiv:1711.00314 [astro-ph.HE], [Astrophys. J. Lett.852,L25(2018)].
- Ropke, G., Blaschke, D., and Schulz, H. (1986). Pauli Quenching Effects in a Simple String Model of Quark / Nuclear Matter, *Phys. Rev.* **D34**, pp. 3499–3513, doi:10.1103/PhysRevD.34.3499.
- Ruiz, M., Shapiro, S. L., and Tsokaros, A. (2018). GW170817, General Relativistic Magnetohydrodynamic Simulations, and the Neutron Star Maximum Mass, *Phys. Rev.* **D97**, 2, p. 021501, doi:10.1103/PhysRevD.97.021501, arXiv:1711.00473 [astro-ph.HE].
- Schaeffer, R., Zdunik, L., and Haensel, P. (1983). Phase transitions in stellar cores. I - Equilibrium configurations, *A&A* **126**, pp. 121–145.
- Sedrakyan, D. M. and Chubaryan, E. V. (1968a). Internal solution for stationary axially symmetric gravitational fields, *Astrophysics* **4**, pp. 227–233, doi:10.1007/BF01013134.
- Sedrakyan, D. M. and Chubaryan, E. V. (1968b). Stationary axially symmetric gravitational fields, *Astrophysics* **4**, pp. 87–93, doi:10.1007/BF01020005.
- Seidov, Z. F. (1971). The Stability of a Star with a Phase Change in General Relativity Theory, *Soviet Astronomy* **15**, p. 347.
- Shibata, M., Fujibayashi, S., Hotokezaka, K., Kiuchi, K., Kyutoku, K., Sekiguchi, Y., and Tanaka, M. (2017). Modeling GW170817 based on numerical relativity and its implications, *Phys. Rev.* **D96**, 12, p. 123012, doi:10.1103/PhysRevD.96.123012, arXiv:1710.07579 [astro-ph.HE].
- Shibata, M., Zhou, E., Kiuchi, K., and Fujibayashi, S. (2019). Constraint on the maximum mass of neutron stars using GW170817 event, arXiv:1905.03656 [astro-ph.HE].
- Stergioulas, N. and Friedman, J. (1995). Comparing models of rapidly rotating relativistic stars constructed by two numerical methods, *Astrophys. J.* **444**, p. 306, doi:10.1086/175605, arXiv:astro-ph/9411032 [astro-ph].

- Tolman, R. C. (1939). Static solutions of Einstein's field equations for spheres of fluid, *Phys. Rev.* **55**, pp. 364–373, doi:10.1103/PhysRev.55.364.
- Weber, F. and Glendenning, N. K. (1992). Application of the improved Hartle method for the construction of general relativistic rotating neutron star models, *Astrophys. J.* **390**, 2, pp. 541–549, doi:10.1086/171304, : [].
- Weber, F. (1999). *Pulsars as Astrophysical Laboratories for Nuclear and Particle Physics* (Taylor & Francis), ISBN 0750303328, 9780750303323, doi: {10.1201/9780203741719}.
- Yagi, K. and Yunes, N. (2013). I-Love-Q Relations in Neutron Stars and their Applications to Astrophysics, Gravitational Waves and Fundamental Physics, *Phys. Rev. D* **88**, 2, p. 023009, doi:10.1103/PhysRevD.88.023009, arXiv:1303.1528 [gr-qc].
- Yakovlev, D. G., Kaminker, A. D., Gnedin, O. Y., and Haensel, P. (2001). Neutrino emission from neutron stars, *Phys. Rept.* **354**, p. 1, doi:10.1016/S0370-1573(00)00131-9, arXiv:astro-ph/0012122 [astro-ph].
- Yasutake, N., Lastowiecki, R., Benic, S., Blaschke, D., Maruyama, T., and Tatum, T. (2014). Finite-size effects at the hadron-quark transition and heavy hybrid stars, *Phys. Rev. C* **89**, p. 065803, doi:10.1103/PhysRevC.89.065803, arXiv:1403.7492 [astro-ph.HE].
- Zdunik, J. L., Bejger, M., Haensel, P., and Gourgoulhon, E. (2006). Phase transitions in rotating neutron stars cores: back bending, stability, core-quakes and pulsar timing, *Astron. Astrophys.* **450**, pp. 747–758, doi: 10.1051/0004-6361:20054260, arXiv:astro-ph/0509806 [astro-ph].
- Zdunik, J. L. and Haensel, P. (2013). Maximum mass of neutron stars and strange neutron-star cores, *Astron. Astrophys.* **551**, p. A61, doi:10.1051/0004-6361/201220697, arXiv:1211.1231 [astro-ph.SR].